Journal Pre-proof

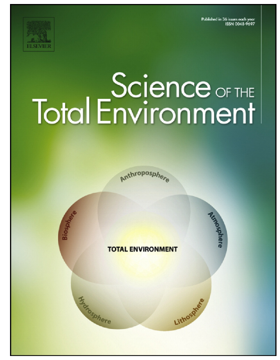

Investigating the efficacy of a fast urban climate model for spatial planning of green and blue spaces for heat mitigation

Jixuan Chen, Peter M. Bach, Kerry A. Nice, João P. Leitão

PII: S0048-9697(24)07082-7

DOI: https://doi.org/10.1016/j.scitotenv.2024.176925

Reference: STOTEN 176925

To appear in: *Science of the Total Environment*

Received date: 4 May 2024

Revised date: 30 September 2024

Accepted date: 12 October 2024

Investigating the efficacy of a fast urban climate model for spatial planning of green and blue spaces for heat mitigation

Jixuan Chen[1)], Peter M. Bach[2)3)]*, Kerry A. Nice[4)], João P. Leitão[1)]

[1)] Swiss Federal Institute of Aquatic Science & Technology (Eawag), Überlandstrasse 133, 8600 Dübendorf ZH, Switzerland

[2)] Institute of Environmental and Process Engineering, Eastern Switzerland University of Applied Sciences (OST), Oberseestrasse 10, 8640 Rapperswil SG, Switzerland

[3)]Department of Civil Engineering, Monash University, Clayton, VIC 3800, Australia[4)] Transport, Health, and Urban Systems Research Lab, Faculty of Architecture, Building, and Planning, University of Melbourne, Melbourne, VIC 3010, Australia

* Corresponding author email: *peterbach@gmail.com*

HIGHLIGHTS

- Investigating the applicability of an efficient urban climate model for planning liveable cities
- Good agreement between TARGET model results and spatially distributed private weather station data
- Sensitivity testing indicates key variables affecting urban heat: canyon shape and concrete parameters
- Substantial air temperature reduction (up to 5.2 °C) with increasing blue-green land cover across city
- Model coupling with pedestrian count data supports people-centric spatial planning of urban spaces

ABSTRACT

Problems caused by urban heat have prompted the exploration of urban greenery and blue spaces for heat mitigation. Various numerical models can simulate heat-related processes, but their use as support-tools to urban planners remains underexplored, particularly at the city-scale, due to high computational demand and complexity of such models. This study investigates the spatial relationships between urban heat, urban form and urban green and blue spaces with the fast climate model TARGET (The Air-temperature Response to

Green/blue-infrastructure Evaluation Tool), which only requires minimal inputs of standard meteorological data, land cover and building geometry data. Using the City of Zurich as our case study, we: (i) validated the TARGET model against air temperature measurements from private sensor networks, (ii) performed a sensitivity analysis to identify key variables affecting urban heat, and (iii) investigated urban heat relationships with blue-green cover at locations frequented by pedestrians. Presence of urban green and blue spaces across the region shows potential for reducing local air temperatures by up to 5.2 °C (with urban forest). Investigating this relationship at different locations in the city revealed key districts that should potentially be targeted for reduction of pedestrian heat-impacts, due to their high pedestrian traffic, fewer green and blue spaces and high daytime air temperatures. Our results not only provide insights into the cooling effect of different amounts of green and blue features in the urban environment, but also demonstrates the application and integration potential of simplified models like TARGET to support the planning of more liveable future cities.

KEYWORDS

urban climate; urban greenery; green spaces; blue spaces; urban planning; model-based planning-support; crowd-sourced data; meteoblue; Netatmo; TARGET

1. INTRODUCTION

The summer of 2024 is confirmed to be the hottest ever recorded since reliable global measurements began, surpassing the previous benchmark set just a year earlier in 2023 (Copernicus, 2024). However, the trend towards more frequent heatwaves due to climate change will continue, regardless of our efforts to mitigate, as warned by the World Metrological Organization (United Nations, 2022). IPCC (2021) reported that the goal to limit global warming below 2 or 1.5 °C is unachievable unless emissions of greenhouse gases are significantly reduced in future decades. In urban settings, extreme heat has negative impacts on human health (Ebi et al., 2021; Nicholls et al., 2008), livelihoods and infrastructure (IPCC, 2022; Topham, 2022). The 2022 heatwave in Europe has resulted in over 60,000 heat-related deaths, estimated from the Eurostat mortality database (Ballester et al., 2023).The economic loss due to heat-induced productivity drop amounts to 0.3 - 0.5% of European GDP historically and is predicted to increase fivefold if no measures are in place by 2060 (García-León et al., 2021). As such, we must prepare for a hotter climate.

Cities are particularly vulnerable to weather extremes and research interest in urban climate has rapidly increased in the past decade with a focus on urban heat and its mitigation (Masson et al., 2020). The negative impacts of heatwaves are exacerbated in cities as a result of rapid urbanisation (Solecki & Marcotullio, 2013). The modification of land cover from natural to artificial materials like concrete and asphalt changes the thermal properties of the urban surface and the urban water cycle (Manoli et al., 2019; Oke, 1987), leading to increased energy storage, reduced evapotranspiration and decreased ventilation. With more than half of the world's population living in urban areas (United Nations, 2019), the capacity of the population and urban services to cope with urban heat has become a major concern. The translation of knowledge from urban climate research to urban planning and policymaking is key to develop practical solutions and alleviate stress on urban environment and populations (Kwok & Ng, 2021).

Research efforts for urban heat mitigation have predominantly focused on innovative pavement designs (Wang et al., 2021), reflective materials (Santamouris & Fiorito, 2021) (should be used with caution as they may negatively impact pedestrian thermal comfort, e.g., Middel et al., 2020; Schneider et al., 2023) and increasing greenery (Wong et al., 2021). It has been demonstrated that one of the best methods for urban outdoor cooling is to increase vegetation cover (Probst et al., 2022). In fact, evapotranspiration from both green and blue spaces is primarily relevant for pedestrian-level air temperature reduction (Gunawardena et al., 2017). While the cooling effects of urban green and blue spaces has been extensively studied by methods of field measurements (Broadbent, Coutts, Tapper, Demuzere, et al., 2018; Skoulika et al., 2014; C. Yu & Hien, 2006) , remote sensing (Gobatti et al., 2023; Vahmani & Jones, 2017; Z. Yu et al., 2017) and numerical modelling (Gromke et al., 2015; Tsoka et al., 2018) at multiple scales (Krayenhoff et al., 2021), spatially explicit city-scale simulation remains rare, and it is yet to be explored utilizing modelling tools to evaluate different scenarios to support city-wide planning of green and blue spaces.

Given the heterogeneity of the urban fabric and function, the local climates across different locations within a city can exhibit significant variability. Understanding how urban heat is distributed over an urban area is important to identify mitigation measures, given limited resources. Numerical modelling, compared to field observations, is a more viable approach to study the interactions between cities and climate, elucidating the role of different processes and facilitating informed urban heat mitigation planning (Oke et al., 2017).

To study urban climate at finer spatial resolutions (< 1 km), energy balance models (e.g. Town Energy Balance TEB: Masson, 2000) have been extensively used until early 2000s, before computational fluid dynamics (CFD) models gained popularity in this research discipline (Toparlar et al., 2017). Perhaps the most popular CFD-based tool used in urban climate studies is ENVI-met (Bruse & Fleer, 1998), which captures all processes of surface-air-vegetation interactions and has been extensively validated in many studies over the last two decades (e.g., Elraouf et al., 2022; Ozkeresteci et al., 2003; Salata et al., 2016). Other CFD models include SOLENE-microclimat, Ansys® Fluent and OpenFOAM® (Matsson, 2023; Musy et al., 2015; Weller et al., 1998). More recently, the large-eddy simulation (LES, a branch of CFD) model PALM-4U (Maronga et al., 2020) has been increasingly used for investigating urban climates at very fine scales (Anders et al., 2023; Geletič et al., 2021). Emerging models like CityFFD (Mortezazadeh et al., 2022) leverages graphics processing units (GPUs) for parallel computation. Despite their prowess, CFD-based models often still require higher computing power and runtime, suffer from improper parameterisation (Bouzouidja et al., 2021) and inaccuracy (Jamei et al., 2019) and are limited to micro- to district-scale simulations due to their complexity. Less complex are models such as RayMan (Matzarakis et al., 2007) and SOLWEIG (Lindberg et al., 2008) that calculate radiation fluxes in urban areas up to neighbourhood-scale, or SUEWS (Järvi et al., 2011a), which models surface energy and hydrological fluxes at local-scale. Despite some authors having claimed that these modelling tools can be used to support planning and ultimately testing of urban heat mitigation options, only a few studies have been presented on this aspect (Alves et al., 2022; Musy et al., 2015). In recent years, with the growing demand for supporting the planning of heat mitigation strategies, more simplified models have been developed, focusing on incorporating representations of trees, vegetation and soil processes. VTUF-3D (K. A. Nice et al., 2018) is an urban microclimate model designed for assessing the effects of green spaces on human thermal comfort. It is detailed and spatially distributed, but still requires high computational cost. The Urban Tethys-Chloris (UT&C) (Meili et al., 2020) is a fully-coupled energy and water balance model that has a strong focus on the biophysics and ecophysiology of vegetation. It is less expensive in terms of computational effort, but due to its 1-D nature, spatial modelling at larger scales remains difficult. The Urban Weather Generator (UWG) (Bueno et al., 2013) couples building energy and urban canyon models and calculates the canopy layer air temperature and humidity. UWG focuses on the urban heat island and is not spatialised in its original form. Assessment of urban heat at higher spatial resolution at district- to city-scale with a more human-centric method is urged (Nazarian et al., 2022). TARGET (Broadbent et al., 2019) is an urban climate modelling tool that builds upon the Local-Scale Urban Meteorological Parameterisation Scheme (LUMPS) (Grimmond & Oke, 2002). It is a rapid spatial model that calculates pedestrian-level air temperatures with minimal inputs and effort in parameter setting. Its representation of urban greenery is through different land cover types, linking directly to the urban form, making it suitable for supporting urban planning practices.

Despite the proposed urban climate models, a very small number of studies has focused on the accuracy of modelling results across city-wide scales (Broadbent et al., 2019), and on the main parameters' influence of modelling results. This can be explained by (i) the complexity of the models and their consequently large computational demand, and (ii) the need for spatially distributed temperature data, which is not frequently available or accessible. As mentioned above, recently proposed, simplified microclimate models, such as TARGET, make city-scale simulations feasible, whereas citizen science and the advent of private sensor networks, e.g. weather stations, create the possibility to assess the validity of urban climate models at a city scale (e.g. Potgieter et al., 2021). Such models also offers potential to assess and improve the walkability (e.g. Jia & Wang, 2021; Mouada et al., 2019) on a city-scale, or to facilitate active transport route choice. The relative simplicity of such models also allows for detailed sensitivity analysis of model parameters to quantify the uncertainty of obtained results.

Based on the few research challenges described above, we address the following research questions in this study:

- Are simplified urban climate models like TARGET able to capture the spatial variability of daytime air temperature in a city?
- What are the important characteristics of the built environment that impacts urban heat?
- How much cooling can green and blue spaces provide in the modelling scheme?
- How can simplified models like TARGET be useful in supporting city-wide planning of green and blue spaces for heat mitigation?

The following study presents methods to enable the effective use of TARGET (our selected model of choice) in supporting urban planning for heat mitigation. We specifically evaluate its performance against spatially-distributed air temperature measurements from private networks and understand, through sensitivity analysis, key model parameters that influence urban heat. With this, we then demonstrate the potential of currently existing urban green and blue spaces across the case study city to mitigate urban heat and how the coupling of urban climate modelling with spatial pedestrian traffic count data can assess and identify opportunities for more strategic and human-centric planning of heat mitigation measures across urban areas.

2. MATERIALS AND METHODS

2.1 Overview of the selected microclimate model

The Air-Temperature Response to Green/blue-infrastructure Evaluation Tool (TARGET) (Broadbent et al., 2019) was developed to be an efficient model to estimate surface temperature and street-level (2 m above ground) air temperature and to assess impacts of urban greenery and water features. TARGET can be applied at specific locations or on a spatial grid (minimum resolution of 30 m recommended for surface temperature and 100 m for air temperature). This section serves as a reiteration of the modelling approaches of the TARGET model. Further specific details of the model are explained in Broadbent et al. (2019) including its individual sub-models for different land cover types.

The model requires three data inputs: (1) land cover, (2) building geometry, and (3) meteorological forcing data. Land cover input should contain fractions of roofs, concrete, road, dry grass, irrigated grass, trees, and water. Average building height and street width for each grid cell are also part of the input data to determine the shape of the urban canyon. Meteorological data (typically from a nearby reference point e.g., an airport or open field) include: *incoming shortwave radiation* (K↓[W m^{-2}]), *incoming longwave radiation* (L↓[W m^{-2}]), *relative humidity* (RH [%]), *air temperature* (T_a [°C]) and *wind speed* (U_z [m s^{-1}]). Longwave radiation can be modelled in TARGET if not available. The meteorological input is used as forcing data for the model, local conditions are simulated based on the influence of the building and urban characteristics. The schematic of TARGET canyon set-up and the structure of TARGET sub-models can be found in Supplementary Information (SI) S1.

TARGET comprises a series of sub-models that calculate the radiation balance, energy balance and, eventually, surface temperature for each surface type with the input meteorological forcing data. At its intended resolution, the shape and density of buildings and vegetation can be generalised into a sky view factor (SVF) for a given mix of urban forms as shown in Eq. (1), and in turn used to calculate available net energy ($R_{n,i}$) that reaches the urban surface of type i, as shown in Eq. (2).

$$SVF = \begin{cases} \left[1+\left(\frac{H}{W^*}\right)^2\right]^{\frac{1}{2}} - \frac{H}{W^*} & for\ ground \\ \frac{1}{2}\left(1+\frac{W^*}{H} - \left[1+\left(\frac{W^*}{H}\right)^2\right]^{\frac{1}{2}}\right) & for\ wall \\ 1 & for\ roof \end{cases} \tag{1}$$

$$R_{n,i} = \left(K\downarrow(1-\alpha_i) + \epsilon_i\left(L\downarrow - \sigma T^4_{surf,i,[t-2]}\right)\right) SVF_i \tag{2}$$

where H is building height [m], W^* is average street width minus tree width [m], α_i is surface albedo [-], ϵ_i is surface emissivity [-], σ is the Stefan-Boltzmann constant (=5.67 × 10^{-8} W m^{-2} K^{-4}), and $T_{surf,i,[t-2]}$ is the modelled surface temperature from two time steps back [°C]. Albedo and emissivity parameters for different land cover types have preset values in TARGET, but can be adjusted by users.

This net energy is then partitioned into components of sensible, latent, and ground storage fluxes according to Eq. (3). The ground storage flux ($Q_{G,i}$) varies through the Objective Hysteresis Model (OHM) (see Grimmond & Oke, 2002) with different coefficient values (a_1, a_2, and a_3) to account for different amounts of heat capacity for different surface types.

$$Q_{G,i} = R_{n,i}a_{1,i} + \left(\frac{\partial R_{n,i}}{\partial t}\right)a_{2,i} + a_{3,i} \quad (3)$$

The force-restore method (Jacobs et al., 2000) is used to calculate the surface temperature change between time steps for each land cover type. As an efficient alternative to the multi-layer conduction method that is commonly used in other climate models, the force-restore method assumes the complex surfaces to be a thin surface layer on top of a deep soil layer, both with uniform vertical temperatures. The calculation then uses a forcing terms driven by the ground flux $Q_{G,i}$ to heat the surface, and a restore term from the deep soil that restrains the forcing term, as written in Eq. (4).

$$\frac{\partial T_{surf,i}}{\partial t} = \frac{Q_{G,i}}{C_i D} - \frac{2\pi}{\tau}\left(T_{surf,i,[t-1]} - T_{m,i,[t-1]}\right) \quad (4)$$

where C_i is the volumetric heat capacity [J m^{-3} K^{-1}], D is the damping depth of the diurnal temperature wave [m], τ is the period (86400 s), and T_m is the average soil temperature [°C], which is calculated using Eq. (5).

$$\frac{\partial T_{m,i}}{\partial t} = \frac{\Delta Q_{G,i}}{C_i D_y} \quad (5)$$

where D_y is the damping depth for the annual temperature cyle (= D√365) [m].

Tree canopy is considered as part of the urban canopy in the model, i.e. trees are modelled at roof height, which allows for a simplified representation of radiation reduction through shading. The surface temperature of trees is assumed to be equal to the meteorological air temperature data, which is proven to be a realistic and efficient estimation (r^2 = 0.98, RMSE = 1.17 °C) (Broadbent, Coutts, Nice, Demuzere, Krayenhoff, et al., 2019). The surface beneath trees is assumed to be representative of ground-level surfaces in the canyon.

There is a separate model that addresses these aspects for water surfaces to ensure reliable results because the OHM-force-restore method tend to substantially over-predict daytime surface water temperatures. The water model resolves the surface energy balance of the water layer considering the absorption of shortwave radiation by water and is designed for small inland water bodies with depths of 0.1 – 1 m.

In the end, for each location (specific point or cell in the grid), surface temperatures are aggregated based on its land cover fractions using Eq. (6). Above-canopy air temperature T_b [°C] is calculated from the meteorological input and wind characteristics. Air temperature is then determined through the surface temperature and T_b by two resistances as shown in Eq. (7). Heat from building walls are taken into account, but anthropogenic heat fluxes are not modelled explicitly.

$$T_{surf} = \sum_{i}^{8}(T_{surf,i}F_i) \tag{6}$$

$$T_{ac} = \frac{\sum_i^7\left(T_{surf,i}c_sF_i\right) + \left[\frac{T_{surf,roof}}{\left(\frac{1}{c_s}+\frac{1}{c_a}\right)}F_{roof}\right] + (T_bc_aW)}{\sum_i^7(c_sF_i) + \left[\frac{F_{roof}}{\left(\frac{1}{c_s}+\frac{1}{c_a}\right)}\right] + (c_aW)} \tag{7}$$

where F_i is the 2-D fractional coverage of surface i in the canyon [-], c_s is the conductance from the surface to the urban canopy layer [m s^{-1}], and c_a is the conductance from the urban canopy layer to the above-canopy layer [m s^{-1}]. Heat transfer from roofs are approximated by two resistances in series.

As part of its development, the model has been validated for a 14-day period for land cover surface temperature at a spatial resolution of 30 m and for a 2-day period for air temperature at a spatial resolution of 100 m. The model is intended for short simulations of days to weeks (i.e. a heatwave) with clear sky conditions and not yet validated for longer period.

The model is carefully designed to balance between simplicity and accuracy with the aim of providing good predictions of street-level air temperature with minimal input and skill requirement. It thus does not account for the horizontal advection, so the predicted cooling impacts of heat mitigation measures are likely to be the maximum potential, which is rather useful for practitioners and policymakers to evaluate different options. The model is open-source and scripted in both Java and Python. Ongoing work involves integrating it to a QGIS plugin that allows direct application and visualisation of modelling results, which will make the model highly accessible to non-expert users.

2.2 Case study description

We selected a study area of 28.8 km^2 spanning the core centre of the City of Zurich in Switzerland (shown in Figure 1) to conduct our study. The area has a diverse land-use composition, with gardens and parks scattered on a principal amount of mixed commercial, offices, and residential zones. Some light industries are located along the major railway and also on the outskirts of the study region. The river of *Limmat* flows through the area from *Lake Zurich*. Two large, vegetated areas north of the river, the *Käferberg* and *Zürichberg* are also included in this study area. Consequently, the area includes all TARGET land cover classes, with the most prevalent being concrete, roof, and irrigated grass, as shown in Figure 1.

On the temporal aspect, to be consistent with the purpose of the model (it is intended for short periods like heatwaves) and, at the same time, provide greater practical value, we selected a short period of warmer temperatures, when a level 3 (considerable danger, daily mean temperature ≥ 25 °C for at least three consecutive days) heat wave warning was issued for lowlands throughout Switzerland. to demonstrate the heat mitigation benefits that greenery can provide during typical hotter days in the City of Zurich in summer.

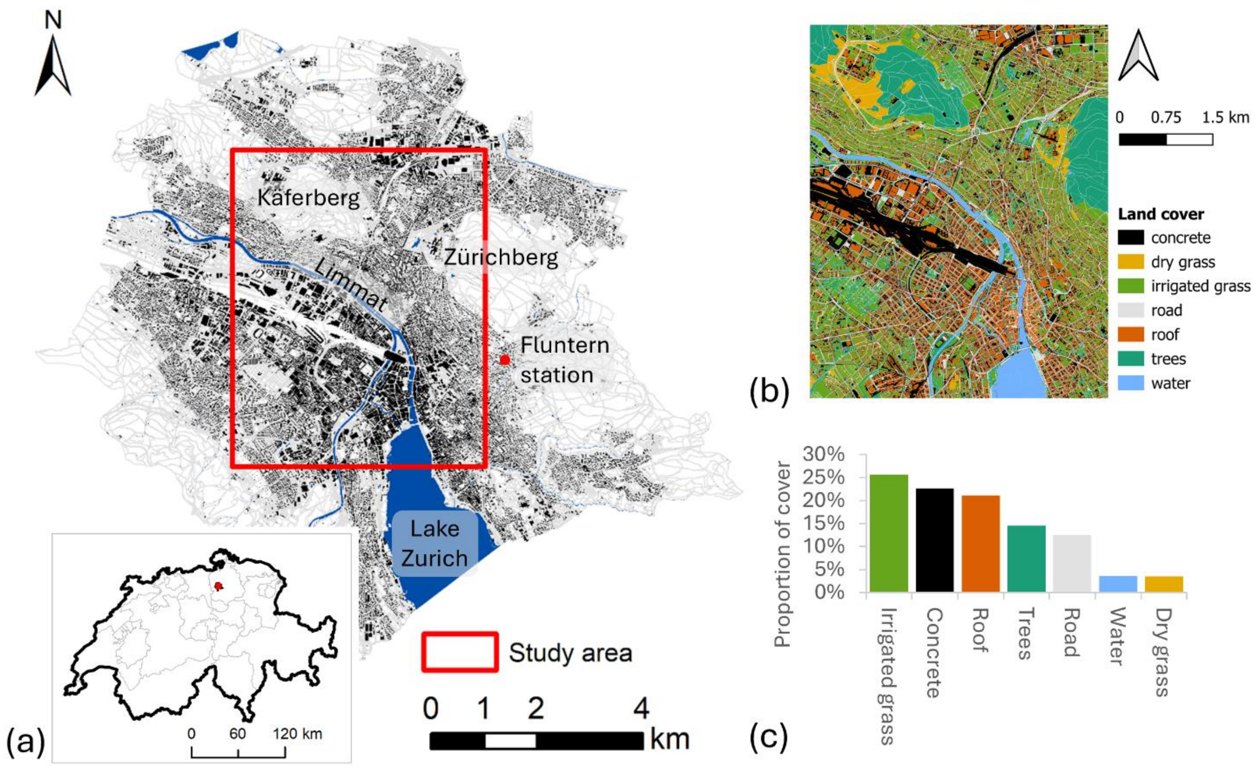

Figure 1. *Location of the selected study area, percentages of TARGET land cover classes in the study area (a – left), land cover map of the study area (b – upper right) and the proportions of land cover types (c – lower right).*

2.3 Data collection and pre-processing

2.3.1 Spatial data

Land cover data were obtained from the local planning authority and resulted from recent official surveying (ARE, 2019). As a pre-processing step, the data were re-classified into the seven land cover types used in the

TARGET model (shown in Figure 1(b) and (c)). Digital surface model (DSM) data of 0.5 m resolution (swisstopo, 2020) was used to calculate building heights and street widths according to (Lindberg et al., 2015). Land cover fractions, building heights, and street widths were aggregated into 100 m grid cells and used as input to the TARGET model.

The global map of local climate zones (LCZs) (Demuzere et al., 2022) was used to group the numerous private weather stations, thus allowing the comparison of model accuracy under different urban environmental conditions.

For demographic indicators, we used pedestrian and bicycle traffic counts gathered by the Zurich civil engineering office (Stadt Zürich, 2023) to describe how frequently different areas are traversed by citizens. There are 20 of automatic counting stations in the study area that count both incoming and outcoming pedestrians and cyclists every 15 minutes. Only one station was kept for one model grid cell of 100 m in the case where multiple stations sit in the same cell, resulting in a total of 18 locations. This study used hourly averaged pedestrian and bicycle count in the warmer hours (12:00 – 18:00) as a metric to judge the traffic volume (see Figure 2(b)) in the post spatial analysis.

2.3.2 Meteorological data

As another input to the TARGET model, meteorological data were obtained from Fluntern meteorological station (556 m a.s.l.) located nearest to the study area (MeteoSwiss, 2023). The data comprises global (shortwave) radiation, incoming longwave radiation, air temperature, relative air humidity, wind speed, and pressure at station level, measured at 10-minute intervals for four days from 2023/07/08 to 2023/07/11. The data were then resampled into 15-minute intervals for to match the temporal resolution of measured data for model evaluation.

To be able to evaluate the spatial output of air temperature results from the model, local air temperature measurements were desired as data from standard weather stations do not have sufficient spatial resolution to be compared with the modelling results. Spatially distributed data from the climate service and data provider meteoblue, which is measured by a quality-controlled Internet of Things (IoT) measurement network (meteoblue, 2024), were available for the City of Zurich. Air temperature measurements at 15-minute intervals from 41 of such stations were obtained for the period studied. Additionally, citizen-contributed data were collected from the company Netatmo, which produces intelligent home devices. One of its featured products is the *Smart Home Weather Station*, a portable instrument that measures indoor and outdoor environments. The users are advised to position the outdoor module half way up the north facing wall of the house, away from any disturbing heating source and avoiding direct sunlight (Netatmo, 2012). A shield can be purchased optionally to protect the station from bad weather and sunlight for more reliable readings. Pictures of the device itself and the shield are provided in SI S2. The outdoor module features an air temperature sensor that has a measurement range of -40 to 65 °C and accuracy of ±0.3 °C. The user can calibrate the temperature manually by adding an offset. This study utilised the outdoor air temperature measurements shared by Netatmo users voluntarily. The data were collected from private Netatmo weather stations within the study area via the Netatmo weather API. A simple quality control of the data combining a simple (Chapman et al., 2017) and an improved method (Napoly et al., 2018) was conducted by filtering out stations that have the same longitude and latitude, removing measurements that deviates more than three standard deviations from the average of measurements from all stations at the same time step, and subsequently discarding data from stations that have missing values. This resulted in a total of 117 stations with continuous data of good quality within the study area, covering the period with available meteorological station data. Locations of the meteoblue and Netatmo stations are shown in Figure 2(a). Measurements were spaced at 30-minute intervals, taken every 15 and 45 minutes after each hour.

2.4 Setup and evaluation of TARGET air temperature results

2.4.1 Model setup

Surface and air temperatures were simulated with TARGET mainly according to (Broadbent et al., 2019), with minor changes in LUMPS coefficients as reflected in the most recent version of the model (K. Nice, 2019). A complete list of parameters used for simulations in this study can be found in Table S3 and the site-specific values in Table S4 in SI. Simulations covered the period of 2023/07/08 until the beginning of 2023/07/12, the first 24 hours being the spin-up period.

2.4.2 Comparison of TARGET results with spatially distributed observations

As mentioned before, to compare TARGET simulation results with both meteoblue and Netatmo data, we grouped these weather stations according to the local climate zone they sit in. The modelled results were still compared to measurements one-to-one for each of the meteoblue or Netatmo data point at every simulation time step. The grouping is only a measure to investigate how the model performs in different urban environments and does not attempt to mask any errors. The locations and LCZ groups of the stations are shown in Figure 2(a).

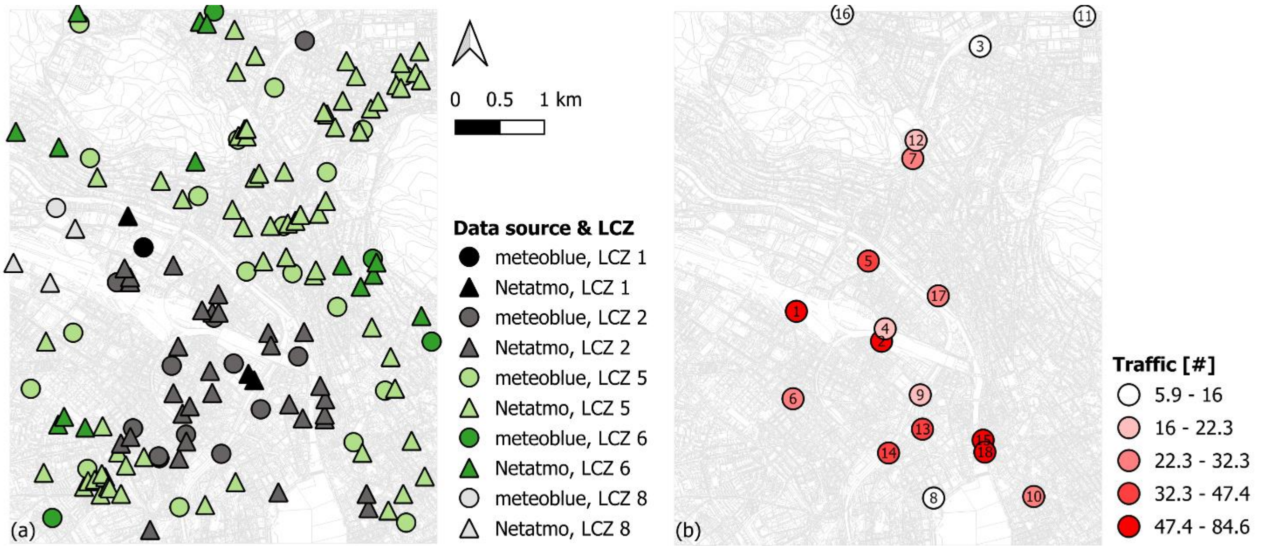

Figure 2. *Agglomerative clustering of meteoblue and Netatmo stations for model validation (a – left) and average hourly pedestrian and bicycle traffic count in the warmer hours (12:00 – 18:00) during the study period (2023/07/09 – 07/11) at 18 counting stations (labelled as 1 – 18) in the study area (b – right).*

2.5 Sensitivity testing of TARGET

A variance-based global sensitivity analysis, or so-called *Sobol sensitivity analysis*, was carried out to better understand the TARGET model itself as well as the uncertainty of the modelling results. The Sobol index indicates the contribution of variance of a parameter to the output variance. It can be estimated by a quasi-Monte Carlo approach, by sampling from parameter ranges, running the sampled values through the model and, finally, determining the sensitivity index by calculating estimators (Saltelli et al., 2010; Sobol, 2001). Separate indices can be calculated for the first-order effect and higher-order interactions between parameters, but this is computationally demanding. Therefore, a total sensitivity index (S_T) was used, which measures the total contribution of a parameter to the output (Y) variance, including any order effects, which is expressed in Equation 8 for parameter i:

$$S_{Ti} = 1 - \frac{Var_{X_i}\left(E_{X_i}(Y|X_i)\right)}{Var(Y)} \tag{8}$$

Among TARGET parameters, the four related to the radiative and thermal properties of the surfaces, including albedo (α), emissivity (ε), thermal diffusivity (κ), and heat capacity (C), were considered worth investigating as they are more accessible for practitioners. We also considered the H/W-ratio of the idealised urban canyon in the sensitivity analysis to better understand the important parameters in modelling the urban environment.

Table 1. *Parameter ranges for Sobol sensitivity analysis.*

Parameter	Range	Sources
α_{roof}	0.08 – 0.70	(Akbari et al., 1992; Oke, 2002)
α_{road}	0.05 – 0.20	(Akbari et al., 1992; Chartered Institution of Building Services Engineers, 2015; Oke, 2002)
α_{conc}	0.10 – 0.35	(Akbari et al., 1992; Chartered Institution of Building Services Engineers, 2015; Oke, 2002)
α_{dry}	0.19 – 0.32	(Chartered Institution of Building Services Engineers, 2015; Järvi et al., 2011b, 2014)
α_{irr}	0.16 – 0.26	(Barry & Chorley, 2009; Chartered Institution of Building Services Engineers, 2015; Järvi et al., 2011b, 2014; Oke, 2002)
α_{veg}	0.05 – 0.20	(Akbari et al., 1992; Barry & Chorley, 2009; Oke, 2002)
ε_{roof}	0.13 – 1.00	(Bitelli et al., 2015; Oke, 2002)
ε_{road}	0.93 – 0.99	(Bitelli et al., 2015; Oke, 2002)
ε_{conc}	0.80 – 0.98	(Bitelli et al., 2015; Oke, 2002; K. Wang et al., 2005)
ε_{dry}	0.88 – 0.99	(Järvi et al., 2011b, 2014; K. Wang et al., 2005)
ε_{irr}	0.90 – 0.98	(Järvi et al., 2011b, 2014; Oke, 2002; Van Wijk, W. R., Scholte Ubing, 1963)
ε_{veg}	0.97 – 0.99	(Järvi et al., 2011b; Oke, 2002)
κ_{roof}	0.05 – 0.57	(Broadbent et al., 2019; Chartered Institution of Building Services Engineers, 2015)
κ_{road}	0.29 – 0.62	(Chartered Institution of Building Services Engineers, 2015; Oke, 2002)
κ_{conc}	0.08 – 1.51	(Chartered Institution of Building Services Engineers, 2015; Oke, 2002)
κ_{dry}	0.11 – 0.32	TARGET default with ± 50% variation
κ_{irr}	0.21 – 0.63	TARGET default with ± 50% variation
C_{roof}	0.81 – 1.96	(Chartered Institution of Building Services Engineers, 2015)
C_{road}	1.70 – 3.91	(Chartered Institution of Building Services Engineers, 2015; Järvi et al., 2011b)
C_{conc}	0.17 – 2.10	(Chartered Institution of Building Services Engineers, 2015)
C_{dry}	0.68 – 2.03	TARGET default with ± 50% variation
C_{irr}	1.10 – 3.29	TARGET default with ± 50% variation
H/W	0.0015 – 5	Representing nearly open space to extremely dense urban environments

α is the surface albedo, ε is the surface emissivity, κ is the thermal diffusivity ($\times10^{-6}$) (m^2 s^{-1}), and C is the volumetric heat capacity ($\times10^{6}$) (J m^{-3} K^{-1}), H/W is the height-to-width ratio of the idealised urban canyon modelled in TARGET.

The Sobol sensitivity analysis was conducted with a single cell with synthetic land cover input consisting of all land cover types in TARGET with equal fractions for a 1-day simulation for 2023/07/09.Variations in parameters were limited by their broadest practical ranges, as in Table 1. For cases where there are few reference values in the literature, TARGET default values were varied by ± 50%. The Sensitivity Analysis Library (SALib) in Python developed by (Herman & Usher, 2017) was utilised for automated analysis. We used a sample size N = 1000 and dimension = 23 for the 23 parameters listed in Table 1. Parameters were sampled by a quasi-random method (Saltelli et al., 2010) which provides a more uniform coverage of the parameter space. Average sensitivity over the day, as well as sensitivity indices at three time stamps across the day, namely 6:00, 14:00 and 22:00, were calculated using Eq. (8), with Y being the overall average air temperature (across the study area and study period) and the air temperature at the selected time stamps averaged over space.

2.6 Evaluation of the impact of blue-green cover on air temperature

An assessment of green and blue cover's impact on air temperature was performed using the simulation results. The green and blue cover of a grid cell was defined to be the fraction of irrigated grass, trees, and water. Grid cells were classified according to their green and blue cover (in %) into five groups and the simulated air temperatures for each group at 6:00, 14:00 and 22:00 on 2023/07/09 were compared using boxplots. The same analysis for surface temperature was performed to complement the results. We also conducted a multiple linear regression (ordinary least squares) to calculate the relationship between land cover characteristics and peak air temperature variability in the study area. Fractions of irrigated grass, trees, and water, separately, were used as the predictor variables and the dependent variable is the air temperature at 14:00 in each model grid cell.

2.7 Combined consideration of temperature, blue-green cover and pedestrian traffic volume

The spatial pedestrian and bicycle traffic data made it possible to prioritise locations within the study area by combining the local air temperature, blue-green cover and the busyness. TARGET-modelled air temperatures at the 18 locations of the traffic counting stations at the hottest time point (14:00) on 2023/09/07 were extracted from the simulation results. The blue-green cover for the corresponding model grid cells were taken from the land cover input and plotted together with air temperature and traffic count data to investigate the impact of greenery on air temperature at sites travelled more frequently and potential for planning heat mitigation strategies.

3. RESULTS AND DISCUSSION

3.1 Evaluation of model performance against measurement data

Figure 3 demonstrates the spatial distribution of TARGET modelled air temperatures at two points in time, at 14:00 and 22:00. The spatial variations are expected: in the afternoon the densely built urban areas are the warmest, and it is cool in the two forested areas, while at night areas that are open and less urban are the coolest, water being a bit warmer than other surfaces. Figure 4 shows the validation of the model for different LCZ groups.

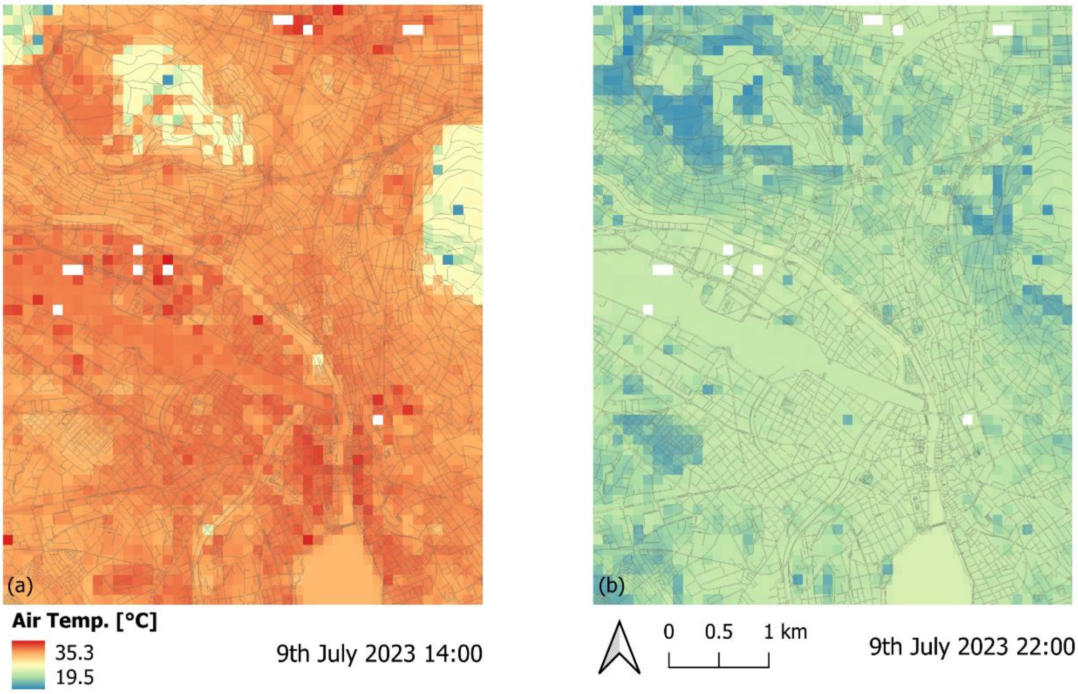

Figure 3. *TARGET modelled air temperature maps (a - left) at 14:00 and (b – right) at 22:00 on 09/07/2023. White areas are cells with a fraction of roof surface higher than 0.75, for which the air temperature was not calculated by TARGET.*

The model generally follows the observed patterns closely, taking meteoblue measurements as representative of the reality. A lag in air temperature change is observed in densely built areas, when compared with modelling results. This lag becomes less prominent with increasing vegetation cover and decreasing building heights as in LCZs 5 and 6, which could be explained by not considering processes of the heat storage and release of urban surfaces in TARGET. Nevertheless, the model still captures the general spatial and temporal patterns of air temperature well, achieving an overall correlation coefficient (r) of 0.95 and an RMSE of 2.2 °C. An all-station point-to-point comparison is provided in Figure S7 in SI.

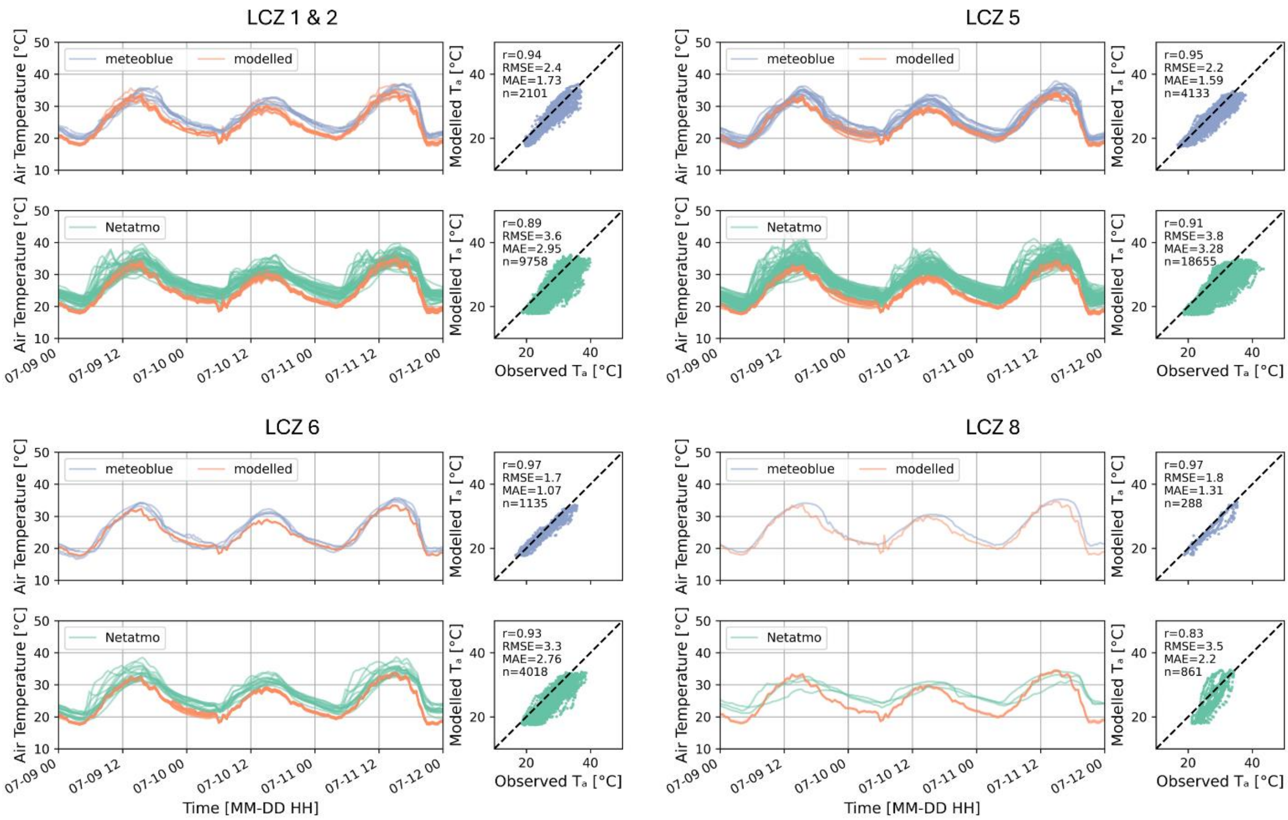

Figure 4. *Comparison of the time series of meteoblue (in purple) and Netatmo (in green) air temperature observations and TARGET modelled air temperature results (in orange) for weather stations sitting in different LCZs. Observed vs. modelled air temperatures are plotted on the right; r is the correlation coefficient, RMSE is the root mean square error [°C], and MAE is the mean absolute error[°C].*

The five LCZ classes present in Figure 2(a) shows a variation of urban environments in the study area from compact high- to mid-rise (LCZs 1 and 2) to open mid- to low- rise (LCZs 5 and 6), where more vegetation is present, and large low-rise (LCZ 8), where the land cover is mostly paved. For LCZs 1 and 8 significantly less data (4 stations in each LCZ) were available; as such, in the results presented in Figure 4 LCZs 1 and 2 were merged but LCZ 8 was kept individually for its lack of similarity to the other classes.

Comparing the results for the four groups in Figure 4, we observed a slight increase in model accuracy (r = 0.94 to 0.97, RMSE = 2.4 to 1.7 °C, MAE = 1.73 to 1.07 °C), comparing against meteoblue data, when the urban environment changes from dense buildings to more open arrangements with higher pervious cover. Similar trend is seen in the results for Netatmo stations, with some deterioration in the performance indicators, which could be explained by the high underlying uncertainty in crowd-sourced data. Higher model accuracy for LCZs 5, 6 and 8 might be attributed to higher presence of these LCZ classes in the validation during the development of the TARGET model, for which data from part of Melbourne (mainly LCZs 6: open low-rise, 8: large low-rise, 4: open high-rise) for land cover surface temperature, and Mawson Lakes (LCZ 8: large low-rise) for canyon surface and air temperature. Another possible reason of such differences in space is that elevations are not considered in TARGET and the model was validated in a flat urban area, while Zurich presents a more hilly landscape. The meteorological station, where the forcing data to drive the model was from, is located approximately 150 m higher than the lowest areas in the middle of the study area where most of the LCZs 1 and 2 stations are located. This may explain why the model underestimates the air temperature the most in the first group and improves as the terrain ascends gradually for LCZs 5 and 6. The same applies for LCZ 8 as this group is the farthest away from the meteorological, where the conditions could differ. Considering the lack of elevation in the representation, the validation results are considered good comparing to the values (r = 0.92, RMSE = 2.0 °C) reported in the original TARGET study (Broadbent et al., 2019) and a more complex model SURFEX (r = 0.94 - 0.95, RMSE = 1.6 – 1.8 °C) (Broadbent, Coutts, Tapper, & Demuzere, 2018) given the simplicity of the model and the comparative nature of the subsequent analyses. Future studies using the model should consider using different meteorological forcings that are representative of different areas, or correcting the modelling results according to elevations.

Comparing measurement data from the two sources, it is obvious that simple quality control could not improve the quality of Netatmo data to the same standard as meteoblue data. Netatmo stations measures warmer daytime temperatures and features a faster warm-up in the morning, which are also seen in (Potgieter et al., 2021), mostly due to the sitting of the stations. Rigorous quality control and filtering methods are yet to be developed to make better use of crowdsourced data (Middel et al., 2022). However, the validation using Netatmo data shows similar trend that was seen in results with meteoblue data, only with deteriorated goodness of fit. Crowdsourced data can still be useful for model validation and other analysis that requires high-resolution spatial atmospheric data, especially when the network is dense and confidence can be increased by averaging.

3.2 Sensitivity testing results

Sensitivity analysis with 22 radiative and thermal parameters for different surfaces plus the H/W-ratio of the canyon shows that the H/W-ratio is dominating in modelling the physics of urban canyon compared to other parameters analysed (see SI S6). The simultaneous change of parameters has led to a maximum variation in the predicted daily and domain average air temperature of 3.6 °C.

We therefore repeated the analysis, leaving out the H/W-ratio, to investigate which land cover types are more important for urban heat. The sensitivity analysis for the 22 physical parameters showed that the heat capacity and thermal diffusivity of concrete are the most sensitive. This indicates that the heat stored in impervious surfaces like concrete is a major contributor to urban heat, confirming the findings from a previous study that daytime air temperature is strongly driven by street fractions (K. A. Nice et al., 2022). A closer look into sensitivities at different time points revealed that, other than concrete parameters, higher sensitivity was found in the thermal properties of dry grass for predicting air temperature in early morning. However, the maximum variation in the average model output when varying these 22 parameters is only 0.07 °C, which is negligible. Since the H/W-ratio is strictly speaking a model input that is calculated based on building geometry data, we believe that it is safe to assume typical values for urban surfaces if these modelling parameters are unknown for a city.

It is worth noting that we consider the physical properties for each surface type individually, so the sensitivity results are limited to the realistic ranges of the parameters for every single surface type. Therefore, these results might not be able to reflect the general importance of a parameter of the overall built environment, such as the average albedo for a neighborhood, although it is well known that albedo is an important factor influencing urban heat (Krayenhoff et al., 2021; L. Wang & Li, 2021).

We have also tested the impact of using input data from different meteorological stations on the modelled air temperature. It was found that stations closer to the study area represents the meteorological conditions within the region better, especially at night-time; More details on theses analyses are presented in SI S5.

3.3 Impact of blue-green cover on urban heat

Figure 5(a) displays the influence of blue-green cover on TARGET surface temperature estimations at different times of the day. The surface temperature difference across different blue-green covers is largest, around 17 °C, in the afternoon. The median surface temperature decreases as blue-green cover increases. This negative relationship is also found in the morning and at night, but with less variability. The significant difference in surface temperatures represents a reduction of around 5.2 °C in air temperature in the afternoon by increasing the blue-green cover from low to high, as depicted in Figure (b).

Previous studies have found surface temperature reductions of 9 – 19 °C provided by green parks (Wong et al., 2021), 11.1 °C by artificial lakes and wetlands (Broadbent, Coutts, Tapper, Demuzere, et al., 2018), and air temperature reductions of 5 °C by water bodies (Murakawa et al., 1991; Peng et al., 2020), 1 – 2 °C provided by urban green spaces (Aram et al., 2019), which is also supported by more recent studies (Cheung et al., 2021; Cheung, Jim, et al., 2022; Cheung, Nice, et al., 2022). Our results are on the right end or even beyond these ranges, because the study area include two large forested areas, *Käferberg* and *Zürichberg*, as described in Section 2.2. These two areas are in fact very different in terms of land cover compositions, compared to mixed urban areas. They consist of over 90% trees, meaning that radiation reaching the ground level is substantially limited. In addition, as the model adds under trees surfaces that are representative of the grid cell land cover composition, additional cooling is expected when the grid cell has high irrigated grass or water fractions other than trees. Therefore, the results show a sudden decrease in surface and air temperatures when increasing the blue-green cover from medium high (MH) to high (H), where all of these forest grid cells belong. If the trend continues without the sudden decrease, the resulting reductions will be well within the reported ranges in the previous studies. The large temperature reductions by trees are expected as studies have shown that urban parks can reduce the air temperature by 0.94 – 5.7 °C (Probst et al., 2022), and that large urban forest can provide a cooling effect of up to 8.4 °C (Yin et al., 2022). Additionally, elevation can also be an influencing factor here, as the degree of greenness is apparently related to the topography of the city. Hence, these locations experience a “double” cooling effect, which can be a reason for the large temperature reductions.

The outliers in surface temperature results can be explained by presence of trees together with other blue-green land covers, which will lead to additional blue-green fractions (bottom outliers), and presence of water (top outliers). Most of the water surfaces present in the study area are natural deep water bodies (*Lake Zurich* and *Limmat* river), violating TARGET’s assumption that water depth is within 1 m. The model sometimes overestimates the air temperature above water, which adds uncertainty to the results.

To summarise, the differences between our modelled results and some of the findings in the literature can be explained by model simplification, different climatic conditions, urban morphology, and urban fabric compositions. Nevertheless, the results show the cooling potential of increasing blue-green cover in urban areas, and that our modelling approach can provide reasonable comparisons of different planning scenarios.

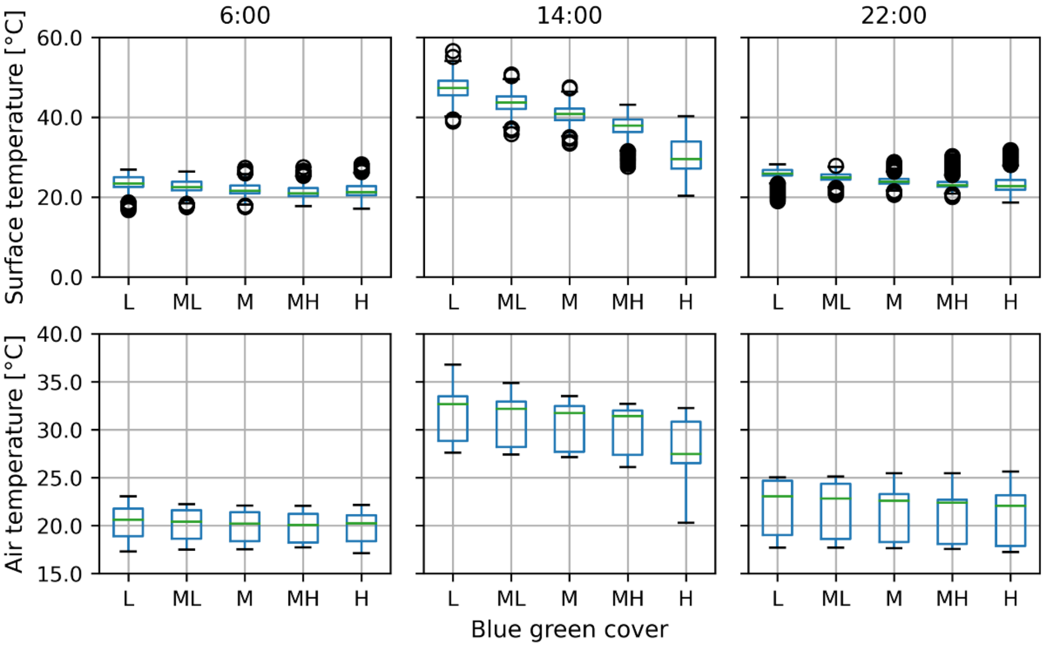

Figure 5. *Boxplots of modelled (upper) surface temperature and (lower) air temperature for grid cells grouped by blue-green cover (L: low, 0-20%, ML: medium low, 20-40%, M: medium, 40-60%, MH: medium high, 60-80%, H: high, 80-100%) at 6:00, 14:00, 22:00 for 2023/07/09 to 2023/07/11.*

To quantify how blue-green land covers contribute to peak air temperature variability, we conducted a multiple linear regression of fractions of irrigated grass, trees and water, and the results are shown in Table 2. The statistical analysis suggests that trees have the largest impact among the three land cover types, which confirms with the results in Figure 5 where temperature drops significantly when large amounts of trees are present. Trees are about two times as effective as irrigated grass in providing cooling, while irrigated grass and water have similar impacts. However, the cooling impact of water is likely underestimated because of the issue with the TARGET water sub-model assumption discussed before.

Table 2. *Peak daytime air temperature multiple linear regression model results.*

Variable	Coefficient [°C]	Standard error	*t* value	*p* value
Intercept	31.99	0.04	721.56	0.000
% irrigated grass	-2.25	0.12	-19.68	0.000

% trees	-4.68	0.10	-47.20	0.000
% water	-2.08	0.17	-12.4	0.000

The kind of analysis presented in this section can help practitioners understand approximately how much cooling impacts they can expect from each type of blue or green land cover in their particular geographical location. This prior knowledge may assist them in designing urban blue and green spaces more effectively.

3.4 Investigating modelled spatial cooling effects of urban greenery and blue spaces

Figure 6incorporates the blue-green cover, air temperature and pedestrian traffic busyness at 18 locations across the City of Zurich at 14:00 on a warm day (2023/07/09), and demonstrates how TARGET can be used to pinpoint priority areas for increasing urban greenery. Places with high blue-green cover unsurprisingly exhibit lower temperatures compared to those with less green and blue spaces. For example, in Figure 6, location 18 is on a footpath next to the *Limmat* river very close to the city centre. Blue-green cover here is over 70%, and modelled air temperature is 1.6 °C lower than that on a street leading to the train station in the main commercial area in the district (location 3), where only around 5% street trees are present and the land surface consists mainly of asphalt and concrete. . A decreasing trend in air temperature is observed with increasing blue-green cover, and the negative relationship becomes stronger with higher presence of green and blue spaces, as the modelled air temperature is also influenced by types of impervious land covers that are not shown in this figure. These impervious land covers play an important role as well. It is not always true that places with green and blue features have lower temperatures than those without. For instance, a location with 30% greenery and 70% concrete might be warmer than a location with 100% dry grass.

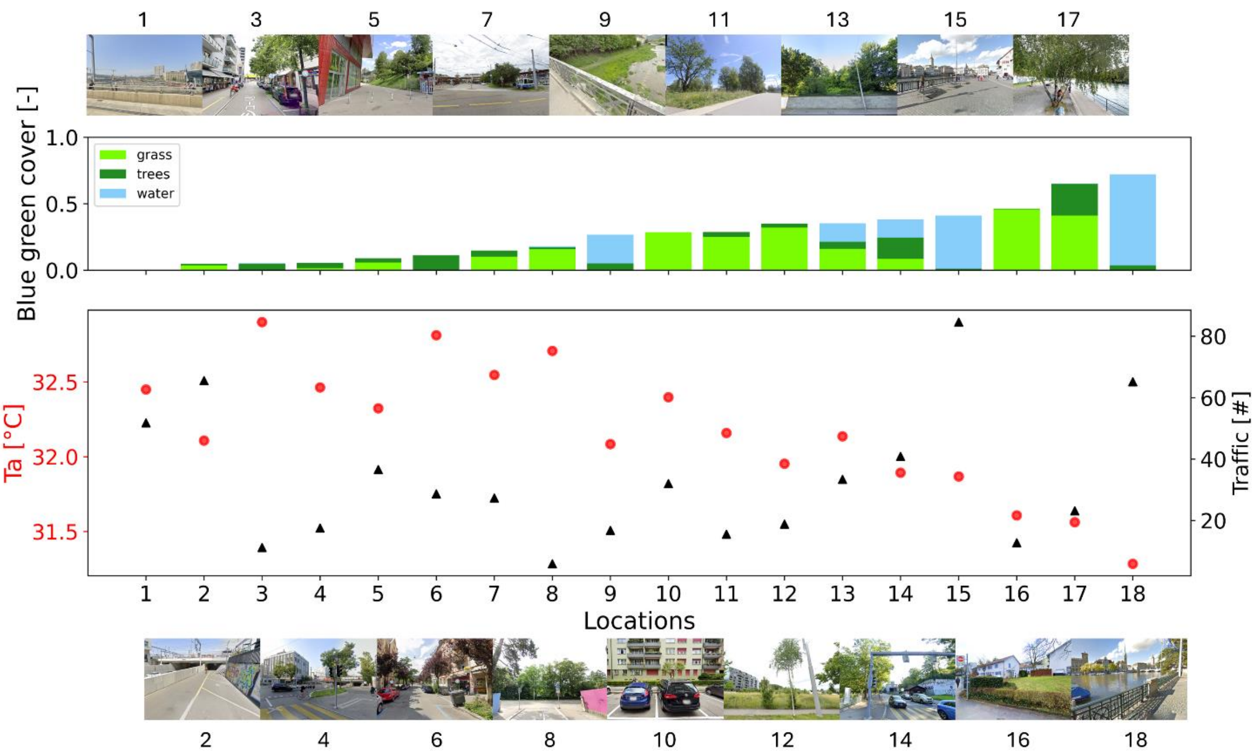

Figure 6. *TARGET modelled air temperatures(extracted from simulation results) at locations 1 – 18 where pedestrian traffic count data are available. The locations are ranked according to their blue-green cover, distinguishing between fractions of irrigated grass, trees and water. Street views at these locations are from Google Maps.*

Based on this type of analysis, urban planners can quickly spot places for improvements from temperature profiles like those presented in Figure 6. Places with high pedestrian and bicycle traffic volume and low blue-green cover are those to be prioritised. To illustrate this idea, location 7 is near *Bucheggplatz*, a transportation hub in Zurich, and it would largely benefit commuters and nearby residents if the pervious cover surrounding the hub can be increased. Another example is location 6 in a rather densely built residential area. Despite some trees on sides of the street, this place appears to have a higher temperature than most of the other locations. Although it can be challenging to alter the land surface considering the already tight space, improvements should certainly be sought. The same applies to location 2 on *Langstrasse*, one of the liveliest streets in the city. Identifying locations like these forms a starting point for urban planners to develop plans and assess proposed greening options by modifying the land cover and simulating new modelling conditions. They can even plan for connected green spaces along the routes and throughout the city to maximise cooling (Gunawardena et al., 2017; Zhang et al., 2017).

As the placement of green features is found to be more opportunistic than strategically planned (Kuller et al., 2021), and planning practitioners are willing to adopt novel planning tools (Kuller et al., 2022), TARGET, together with post-spatial analysis, can fit in this purpose very well. The methods we proposed and demonstrated in this study are easy to adopt, fast to process, and operable at a city-scale. The model is also highly flexible to simulate the cooling impact of different greenery options including types, locations and even maintenance level (by switching between dry and wet grass), under different climate conditions (past, present or future) and in different places. Modelling results can be coupled with different data, not necessarily traffic, to evaluate heat mitigation options with consideration of other factors according to user preferences. It is also possible to implement a multi-criteria decision analysis (MCDA) approach starting with the idea presented in this paper.

3.5 Limitations of the proposed approach

We demonstrated a range of applications that TARGET can be used to support the planning of urban microclimate. Although TARGET was the specific tool used, the overall methodology could utilise any suitable simplified climate model. Nevertheless, several limitations remain that future work can address.

TARGET's design represents a trade-off between speed and level of detail to support planners in evaluating suburb- to city-scale blue-green infrastructure solutions and test heat mitigation scenarios. As such, it aims to generate reliable temperature estimations while maintaining computational efficiency and consequently makes several key assumptions. One crucial assumption of TARGET is that it does not consider horizontal advection (Broadbent et al., 2019). In reality, the local cooling impact of these infrastructures is weakened by atmospheric mixing, which is particularly strong when wind speed is high (Broadbent et al., 2019). Without proper representation of the horizontal mixing of air in the model, the predicted cooling benefits of greenery in this study would most likely be the maximum value.

In addition, as mentioned before, the water sub-model of TARGET is not designed for natural lakes and rivers, which were present in the case study; this sometimes leads to instability in the air temperature results above these water surfaces. Variation of elevation is not accounted for in the model. This simplification could lead to errors in air temperature results for the case study. These are limitations we acknowledge and worked with throughout our analysis.

4. CONCLUSION

This study reports insights into modelling air temperature with an urban climate model called TARGET to assess the impacts of green and blue spaces and plan liveable cities. We compared TARGET results with local air temperature measurements from professional climate service and data provider and crowd-sourced data from home devices, and also conducted a parameter sensitivity analysis for the model. Finally, we demonstrated how TARGET results can be used to support spatial planning of green and blue spaces in cities to improve city liveability. The study found that city-wide modelling with TARGET generally captures the air temperature patterns well (r = 0.95, RMSE = 2.2°C). Additionally, we demonstrated the added value of spatially distributed temperature data from private sensor networks to validate urban climate models. Based on the sensitivity testing results, the canyon height-to-width ratio was found to be the most influential on urban heat, and concrete parameters had more impact on the results than other surfaces' parameters. Application of the model to the case study of Zurich found that an air temperature reduction of around 1.2 °C can be achieved by increasing the blue-green cover of a location from low (0 – 20%) to medium high (60 – 80%), and a further 4 °C if the location is transformed to an urban forest, which are in accordance with literature values and confirms the validity of the predicted cooling impact provided by increasing green and blue spaces. Notably, we showed that TARGET is useful for identifying critical locations for urban heat mitigation when coupled with spatial pedestrian count data.

In summary, we found that TARGET is a useful tool to simulate air temperature fast and accurately at city-scale, allowing urban planners to: (1) identify locations for improvements by looking for low blue-green cover and high temperature, (2) assess different planning options simply by altering the land covers and run TARGET with the new land cover input, (3) couple TARGET results with different spatial data for multi-faceted analyses. The framework around quick and efficient model setup and simulation we presented in this study is generalisable to other locations and offers opportunity for urban planners to use simplified models for improving the liveability in cities.

Code and data availability. TARGET is distributed under the Creative Commons Attribution-NonCommercial-ShareAlike 4.0 Generic (CC BY-NC-SA 4.0). Python code used for this study is available at https://github.com/jixuan-chen/target.

ACKNOWLEDGEMENTS

This work was funded by the Swiss National Science Foundation (SNSF) Project 200021_201029: *Heat-Down – Integrated Modelling of Stormwater and Urban Heat for cooling Cities*. We would also like to thank Christian Förster for his assistance in scripts for the data mining of crowd-sourced temperature measurements.

REFERENCES

Akbari, H., Davis, S., Dorsano, S., Huang, J., & Winnett, S. (Eds.). (1992). *Cooling our Communities—A Guidebook On Tree Planting And Light Colored Surfacing*. US Environmental Protection Agency.

Alves, F. M., Gonçalves, A., & Del Caz-Enjuto, M. R. (2022). The Use of Envi-Met for the Assessment of Nature-Based Solutions' Potential Benefits in Industrial Parks—A Case Study of Argales Industrial Park (Valladolid, Spain). *Infrastructures*, *7*(6), 85. https://doi.org/10.3390/infrastructures7060085

Amt für Raumentwicklung Zürich. (2019). *AV - Bodenbedeckung*.

Anders, J., Schubert, S., Sauter, T., Tunn, S., Schneider, C., & Salim, M. (2023). Modelling the impact of an urban development project on microclimate and outdoor thermal comfort in a mid-latitude city. *Energy and Buildings*, *296*, 113324. https://doi.org/10.1016/j.enbuild.2023.113324

Aram, F., Higueras García, E., Solgi, E., & Mansournia, S. (2019). Urban green space cooling effect in cities. *Heliyon*, *5*(4), e01339. https://doi.org/10.1016/j.heliyon.2019.e01339

Ballester, J., Quijal-Zamorano, M., Méndez Turrubiates, R. F., Pegenaute, F., Herrmann, F. R., Robine, J. M., Basagaña, X., Tonne, C., Antó, J. M., & Achebak, H. (2023). Heat-related mortality in Europe during the summer of 2022. *Nature Medicine*. https://doi.org/10.1038/s41591-023-02419-z

Barry, R. G., & Chorley, R. J. (2009). *Atmosphere, Weather and Climate* (8th ed.). Routledge.

Bitelli, G., Conte, P., Csoknyai, T., Franci, F., Girelli, V. A., & Mandanici, E. (2015). Aerial thermography for energetic modelling of cities. *Remote Sensing*, *7*(2), 2152–2170. https://doi.org/10.3390/rs70202152

Bouzouidja, R., Cannavo, P., Bodénan, P., Gulyás, Á., Kiss, M., Kovács, A., Béchet, B., Chancibault, K., Chantoiseau, E., Bournet, P.-E., Bouzidi, R., Guénon, R., Lebeau, T., Musy, M., & Rodriguez, F. (2021). How to evaluate nature-based solutions performance for microclimate, water and soil management issues – Available tools and methods from Nature4Cities European project results. *Ecological Indicators*, *125*, 107556. https://doi.org/10.1016/j.ecolind.2021.107556

Broadbent, A. M., Coutts, A. M., Nice, K. A., Demuzere, M., Krayenhoff, E. S., Tapper, N. J., & Wouters, H. (2019). The Air-temperature Response to Green/blue-infrastructure Evaluation Tool (TARGET v1.0):

An efficient and user-friendly model of city cooling. *Geoscientific Model Development*, *12*(2), 785–803. https://doi.org/10.5194/gmd-12-785-2019

Broadbent, A. M., Coutts, A. M., Tapper, N. J., & Demuzere, M. (2018). The cooling effect of irrigation on urban microclimate during heatwave conditions. *Urban Climate*, *23*, 309–329. https://doi.org/10.1016/j.uclim.2017.05.002

Broadbent, A. M., Coutts, A. M., Tapper, N. J., Demuzere, M., & Beringer, J. (2018). The microscale cooling effects of water sensitive urban design and irrigation in a suburban environment. *Theoretical and Applied Climatology*, *134*(1–2), 1–23. https://doi.org/10.1007/s00704-017-2241-3

Bruse, M., & Fleer, H. (1998). Simulating surface-plant-air interactions inside urban environments with a three dimensional numerical model. *Environmental Modelling and Software*, *13*(3–4), 373–384. https://doi.org/10.1016/S1364-8152(98)00042-5

Bueno, B., Norford, L., Hidalgo, J., & Pigeon, G. (2013). The urban weather generator. *Journal of Building Performance Simulation*, *6*(4), 269–281. https://doi.org/10.1080/19401493.2012.718797

Chapman, L., Bell, C., & Bell, S. (2017). Can the crowdsourcing data paradigm take atmospheric science to a new level? A case study of the urban heat island of London quantified using Netatmo weather stations. *International Journal of Climatology*, *37*(9), 3597–3605. https://doi.org/10.1002/joc.4940

Chartered Institution of Building Services Engineers. (2015). *Enviromental Design: CIBSE Guide A*. CIBSE.

Cheung, P. K., Jim, C. Y., Tapper, N., Nice, K. A., & Livesley, S. J. (2022). Daytime irrigation leads to significantly cooler private backyards in summer. *Urban Climate*, *46*, 101310. https://doi.org/10.1016/j.uclim.2022.101310

Cheung, P. K., Livesley, S. J., & Nice, K. A. (2021). Estimating the cooling potential of irrigating green spaces in 100 global cities with arid, temperate or continental climates. *Sustainable Cities and Society*, *71*, 102974. https://doi.org/10.1016/j.scs.2021.102974

Cheung, P. K., Nice, K. A., & Livesley, S. J. (2022). Irrigating urban green space for cooling benefits: The mechanisms and management considerations. *Environmental Research: Climate*, *1*(1), 015001. https://doi.org/10.1088/2752-5295/ac6e7c

Copernicus. (2024, September 6). *Copernicus: Summer 2024 – Hottest on record globally and for Europe*. https://climate.copernicus.eu/copernicus-summer-2024-hottest-record-globally-and-europe

Demuzere, M., Kittner, J., Martilli, A., Mills, G., Moede, C., Stewart, I. D., van Vliet, J., & Bechtel, B. (2022). A global map of local climate zones to support earth system modelling and urban-scale environmental science. *Earth System Science Data*, *14*(8), 3835–3873. https://doi.org/10.5194/essd-14-3835-2022

Ebi, K. L., Capon, A., Berry, P., Broderick, C., de Dear, R., Havenith, G., Honda, Y., Kovats, R. S., Ma, W., Malik, A., Morris, N. B., Nybo, L., Seneviratne, S. I., Vanos, J., & Jay, O. (2021). Hot weather and heat extremes: Health risks. *The Lancet*, *398*(10301), 698–708. https://doi.org/10.1016/S0140-6736(21)01208-3

Elraouf, R. A., ELMokadem, A., Megahed, N., Eleinen, O. A., & Eltarabily, S. (2022). Evaluating urban outdoor thermal comfort: A validation of ENVI-met simulation through field measurement. *Journal of Building Performance Simulation*, *15*(2), 268–286. https://doi.org/10.1080/19401493.2022.2046165

García-León, D., Casanueva, A., Standardi, G., Burgstall, A., Flouris, A. D., & Nybo, L. (2021). Current and projected regional economic impacts of heatwaves in Europe. *Nature Communications*, *12*(1), 5807. https://doi.org/10.1038/s41467-021-26050-z

Geletič, J., Lehnert, M., Krč, P., Resler, J., & Krayenhoff, E. S. (2021). High-Resolution Modelling of Thermal Exposure during a Hot Spell: A Case Study Using PALM-4U in Prague, Czech Republic. *Atmosphere*, *12*(2), 175. https://doi.org/10.3390/atmos12020175

Gobatti, L., Bach, P. M., Scheidegger, A., & Leitão, J. P. (2023). Using satellite imagery to investigate Blue-Green Infrastructure establishment time for urban cooling. *Sustainable Cities and Society*, *97*, 104768. https://doi.org/10.1016/j.scs.2023.104768

Grimmond, C. S. B., & Oke, T. R. (1991). An evapotranspiration-interception model for urban areas. *Water Resources Research*, *27*(7), 1739–1755. https://doi.org/10.1029/91WR00557

Grimmond, C. S. B., & Oke, T. R. (2002). Turbulent Heat Fluxes in Urban Areas: Observations and a Local-Scale Urban Meteorological Parameterization Scheme (LUMPS). *Journal of Applied Meteorology*, *41*(7), 792–810. https://doi.org/10.1175/1520-0450(2002)041<0792:THFIUA>2.0.CO;2

Gromke, C., Blocken, B., Janssen, W., Merema, B., van Hooff, T., & Timmermans, H. (2015). CFD analysis of transpirational cooling by vegetation: Case study for specific meteorological conditions during a heat wave in Arnhem, Netherlands. *Building and Environment*, *83*, 11–26. https://doi.org/10.1016/j.buildenv.2014.04.022

Gunawardena, K. R., Wells, M. J., & Kershaw, T. (2017). Utilising green and bluespace to mitigate urban heat island intensity. *Science of The Total Environment*, *584–585*, 1040–1055. https://doi.org/10.1016/j.scitotenv.2017.01.158

Herman, J., & Usher, W. (2017). SALib: An open-source Python library for Sensitivity Analysis. *The Journal of Open Source Software*, *2*(9), 97. https://doi.org/10.21105/joss.00097

IPCC. (2021). *Climate change 2021: The physical science basis. Contribution of Working Group I to the Sixth Assessment Report of the Intergovernmental Panel on Climate Change*. Cambridge University Press Cambridge, UK.

IPCC. (2022). *Summary for Policymakers*. Cambridge University Press. https://www.ipcc.ch/report/ar6/wg2/downloads/report/IPCC_AR6_WGII_SummaryForPolicymakers.pdf

Jacobs, A. F. G., Heusinkveld, B. G., & Berkowicz, S. M. (2000). Force-restore technique for ground surface temperature and moisture content in a dry desert system. *Water Resources Research*, *36*(5), 1261–1268. https://doi.org/10.1029/2000WR900016

Jamei, E., Seyedmahmoudian, M., Horan, B., & Stojcevski, A. (2019). Verification of a bioclimatic modeling system in a growing suburb in Melbourne. *Science of the Total Environment*, *689*, 883–898. https://doi.org/10.1016/j.scitotenv.2019.06.399

Järvi, L., Grimmond, C. S. B., & Christen, A. (2011a). The Surface Urban Energy and Water Balance Scheme (SUEWS): Evaluation in Los Angeles and Vancouver. *Journal of Hydrology*, *411*(3–4), 219–237. https://doi.org/10.1016/j.jhydrol.2011.10.001

Järvi, L., Grimmond, C. S. B., & Christen, A. (2011b). The Surface Urban Energy and Water Balance Scheme (SUEWS): Evaluation in Los Angeles and Vancouver. *Journal of Hydrology*, *411*(3–4), 219–237. https://doi.org/10.1016/j.jhydrol.2011.10.001

Järvi, L., Grimmond, C. S. B., Taka, M., Nordbo, A., Setälä, H., & Strachan, I. B. (2014). Development of the Surface Urban Energy and Water Balance Scheme (SUEWS) for cold climate cities. *Geoscientific Model Development*, *7*(4), 1691–1711. https://doi.org/10.5194/gmd-7-1691-2014

Jia, S., & Wang, Y. (2021). Effect of heat mitigation strategies on thermal environment, thermal comfort, and walkability: A case study in Hong Kong. *Building and Environment*, *201*, 107988. https://doi.org/10.1016/j.buildenv.2021.107988

Krayenhoff, E. S., Broadbent, A. M., Zhao, L., Georgescu, M., Middel, A., Voogt, J. A., Martilli, A., Sailor, D. J., & Erell, E. (2021). Cooling hot cities: A systematic and critical review of the numerical modelling literature. *Environmental Research Letters*, *16*(5), 053007. https://doi.org/10.1088/1748-9326/abdcf1

Kuller, M., Farrelly, M., Marthanty, D. R., Deletic, A., & Bach, P. M. (2022). Planning support systems for strategic implementation of nature-based solutions in the global south: Current role and future potential in Indonesia. *Cities*, *126*, 103693. https://doi.org/10.1016/j.cities.2022.103693

Kuller, M., Reid, D. J., & Prodanovic, V. (2021). Are we planning blue-green infrastructure opportunistically or strategically? Insights from Sydney, Australia. *Blue-Green Systems*, *3*(1), 267–280. https://doi.org/10.2166/bgs.2021.023

Kwok, Y. T., & Ng, E. Y. Y. (2021). Trends, topics, and lessons learnt from real case studies using mesoscale atmospheric models for urban climate applications in 2000–2019. *Urban Climate*, *36*, 100785. https://doi.org/10.1016/j.uclim.2021.100785

Lindberg, F., Grimmond, C. S. B., & Martilli, A. (2015). Sunlit fractions on urban facets – Impact of spatial resolution and approach. *Urban Climate*, *12*, 65–84. https://doi.org/10.1016/j.uclim.2014.11.006

Lindberg, F., Holmer, B., & Thorsson, S. (2008). SOLWEIG 1.0—Modelling spatial variations of 3D radiant fluxes and mean radiant temperature in complex urban settings. *International Journal of Biometeorology*, *52*(7), 697–713. https://doi.org/10.1007/s00484-008-0162-7

Manoli, G., Fatichi, S., Schläpfer, M., Yu, K., Crowther, T. W., Meili, N., Burlando, P., Katul, G. G., & Bou-Zeid, E. (2019). Magnitude of urban heat islands largely explained by climate and population. *Nature*, *573*(7772), 55–60. https://doi.org/10.1038/s41586-019-1512-9

Maronga, B., Banzhaf, S., Burmeister, C., Esch, T., Forkel, R., Fröhlich, D., Fuka, V., Gehrke, K. F., Geletič, J., Giersch, S., Gronemeier, T., Groß, G., Heldens, W., Hellsten, A., Hoffmann, F., Inagaki, A., Kadasch, E., Kanani-Sühring, F., Ketelsen, K., … Raasch, S. (2020). Overview of the PALM model system 6.0. *Geoscientific Model Development*, *13*(3), 1335–1372. https://doi.org/10.5194/gmd-13-1335-2020

Masson, V. (2000). A Physically-Based Scheme For The Urban Energy Budget In Atmospheric Models. *Boundary-Layer Meteorology*, *94*(3), 357–397. https://doi.org/10.1023/A:1002463829265

Masson, V., Lemonsu, A., Hidalgo, J., & Voogt, J. (2020). Urban Climates and Climate Change. *Annual Review of Environment and Resources*, *45*(1), 411–444. https://doi.org/10.1146/annurev-environ-012320-083623

Matsson, J. E. (2023). *An introduction to ansys fluent 2023*. Sdc Publications.

Matzarakis, A., Rutz, F., & Mayer, H. (2007). Modelling radiation fluxes in simple and complex environments—Application of the RayMan model. *International Journal of Biometeorology*, *51*(4), 323–334. https://doi.org/10.1007/s00484-006-0061-8

Meili, N., Manoli, G., Burlando, P., Bou-Zeid, E., Chow, W. T. L., Coutts, A. M., Daly, E., Nice, K. A., Roth, M., Tapper, N. J., Velasco, E., Vivoni, E. R., & Fatichi, S. (2020). An urban ecohydrological model to quantify the effect of vegetation on urban climate and hydrology (UT&C v1.0). *Geoscientific Model Development*, *13*(1), 335–362. https://doi.org/10.5194/gmd-13-335-2020

meteoblue. (2024). *Measure urban climate where it matters with modern IoT technology*. Meteoblue. https://content.meteoblue.com/en/business-solutions/meteo-climate-services/city-climate/iot-station-network/

MeteoSwiss. (2023). *Automatic measurement network*. https://www.meteoswiss.admin.ch/weather/measurement-systems/land-based-stations/automatic-measurement-network.html

Middel, A., Nazarian, N., Demuzere, M., & Bechtel, B. (2022). Urban Climate Informatics: An Emerging Research Field. *Frontiers in Environmental Science*, *10*. https://doi.org/10.3389/fenvs.2022.867434

Middel, A., Turner, V. K., Schneider, F. A., Zhang, Y., & Stiller, M. (2020). Solar reflective pavements—A policy panacea to heat mitigation? *Environmental Research Letters*, *15*(6), 064016. https://doi.org/10.1088/1748-9326/ab87d4

Mortezazadeh, M., Wang, L. L., Albettar, M., & Yang, S. (2022). CityFFD – City fast fluid dynamics for urban microclimate simulations on graphics processing units. *Urban Climate*, *41*, 101063. https://doi.org/10.1016/j.uclim.2021.101063

Mouada, N., Zemmouri, N., & Meziani, R. (2019). Urban morphology, outdoor thermal comfort and walkability in hot, dry cities: Case study in Sidi Okba, Algeria. *International Review for Spatial Planning and Sustainable Development*, *7*(1), 117–133. https://doi.org/10.14246/irspsda.7.1_117

Murakawa, S., Sekine, T., Narita, K., & Nishina, D. (1991). Study of the effects of a river on the thermal environment in an urban area. *Energy and Buildings*, *16*(3), 993–1001. https://doi.org/10.1016/0378-7788(91)90094-J

Musy, M., Malys, L., Morille, B., & Inard, C. (2015). The use of SOLENE-microclimat model to assess adaptation strategies at the district scale. *Urban Climate*, *14*, 213–223. https://doi.org/10.1016/j.uclim.2015.07.004

Napoly, A., Grassmann, T., Meier, F., & Fenner, D. (2018). Development and Application of a Statistically-Based Quality Control for Crowdsourced Air Temperature Data. *Frontiers in Earth Science*, *6*. https://www.frontiersin.org/articles/10.3389/feart.2018.00118

Nazarian, N., Krayenhoff, E. S., Bechtel, B., Hondula, D. M., Paolini, R., Vanos, J., Cheung, T., Chow, W. T. L., de Dear, R., Jay, O., Lee, J. K. W., Martilli, A., Middel, A., Norford, L. K., Sadeghi, M., Schiavon, S., & Santamouris, M. (2022). Integrated Assessment of Urban Overheating Impacts on Human Life. *Earth's Future*, *10*(8), e2022EF002682. https://doi.org/10.1029/2022EF002682

Netatmo. (2012). *Netatmo user manual*. https://static.netatmo.com/station/faq_en-US.pdf

Nice, K. (2019). Mothlight / target_java. *Bitbucket Repository*. https://bitbucket.org/mothlight/target_java/src/master/

Nice, K. A., Coutts, A. M., & Tapper, N. J. (2018). Development of the VTUF-3D v1.0 urban micro-climate model to support assessment of urban vegetation influences on human thermal comfort. *Urban Climate*, *24,* 1052–1076. https://doi.org/10.1016/j.uclim.2017.12.008

Nice, K. A., Nazarian, N., Lipson, M. J., Hart, M. A., Seneviratne, S., Thompson, J., Naserikia, M., Godic, B., & Stevenson, M. (2022). Isolating the impacts of urban form and fabric from geography on urban heat and human thermal comfort. *Building and Environment*, *224*, 109502. https://doi.org/10.1016/j.buildenv.2022.109502

Nicholls, N., Skinner, C., Loughnan, M., & Tapper, N. (2008). A simple heat alert system for Melbourne, Australia. *International Journal of Biometeorology*, *52*(5), 375–384. https://doi.org/10.1007/s00484-007-0132-5

Oke, T. R. (1987). *Boundary layer climates* (Second edition). Routledge.

Oke, T. R. (2002). *Boundary Layer Climates.* (2nd ed.). Routledge.

Oke, T. R., Mills, G., Christen, A., & Voogt, J. A. (2017). *Urban Climates*. Cambridge University Press. https://doi.org/10.1017/9781139016476

Ozkeresteci, I., Crewe, K., Brazel, A. J., & Bruse, M. (2003). *Use and Evaluation of the Envi-Met Model for Environmental Design and Planning: An Experiment on Linear Parks*.

Peng, J., Liu, Q., Xu, Z., Lyu, D., Du, Y., Qiao, R., & Wu, J. (2020). How to effectively mitigate urban heat island effect? A perspective of waterbody patch size threshold. *Landscape and Urban Planning*, *202*, 103873. https://doi.org/10.1016/j.landurbplan.2020.103873

Potgieter, J., Nazarian, N., Lipson, M. J., Hart, M. A., Ulpiani, G., Morrison, W., & Benjamin, K. (2021). Combining High-Resolution Land Use Data With Crowdsourced Air Temperature to Investigate Intra-Urban Microclimate. *Frontiers in Environmental Science*, *9*, 720323. https://doi.org/10.3389/fenvs.2021.720323

Probst, N., Bach, P. M., Cook, L. M., Maurer, M., & Leitão, J. P. (2022). Blue Green Systems for urban heat mitigation: Mechanisms, effectiveness and research directions. *Blue-Green Systems*, *4*(2), 348–376. https://doi.org/10.2166/bgs.2022.028

Salata, F., Golasi, I., De Lieto Vollaro, R., & De Lieto Vollaro, A. (2016). Urban microclimate and outdoor thermal comfort. A proper procedure to fit ENVI-met simulation outputs to experimental data. *Sustainable Cities and Society*, *26*, 318–343. https://doi.org/10.1016/j.scs.2016.07.005

Saltelli, A., Annoni, P., Azzini, I., Campolongo, F., Ratto, M., & Tarantola, S. (2010). Variance based sensitivity analysis of model output. Design and estimator for the total sensitivity index. *Computer Physics Communications*, *181*(2), 259–270. https://doi.org/10.1016/j.cpc.2009.09.018

Santamouris, M., & Fiorito, F. (2021). On the impact of modified urban albedo on ambient temperature and heat related mortality. *Solar Energy*, *216*, 493–507. https://doi.org/10.1016/j.solener.2021.01.031

Schneider, F. A., Ortiz, J. C., Vanos, J. K., Sailor, D. J., & Middel, A. (2023). Evidence-based guidance on reflective pavement for urban heat mitigation in Arizona. *Nature Communications*, *14*(1), 1467. https://doi.org/10.1038/s41467-023-36972-5

Skoulika, F., Santamouris, M., Kolokotsa, D., & Boemi, N. (2014). On the thermal characteristics and the mitigation potential of a medium size urban park in Athens, Greece. *Landscape and Urban Planning*, *123*, 73–86. https://doi.org/10.1016/j.landurbplan.2013.11.002

Sobol, I. M. (2001). Global sensitivity indices for nonlinear mathematical models and their Monte Carlo estimates. *Mathematics and Computers in Simulation*, *55*(1–3), 271–280. https://doi.org/10.1016/S0378-4754(00)00270-6

Solecki, W., & Marcotullio, P. J. (2013). Climate Change and Urban Biodiversity Vulnerability. In T. Elmqvist, M. Fragkias, J. Goodness, B. Güneralp, P. J. Marcotullio, R. I. McDonald, S. Parnell, M. Schewenius, M. Sendstad, K. C. Seto, & C. Wilkinson (Eds.), *Urbanization, Biodiversity and Ecosystem Services: Challenges and Opportunities* (pp. 485–504). Springer Netherlands. https://doi.org/10.1007/978-94-007-7088-1_25

Stadt Zürich. (2023). *Daten der automatischen Fussgänger- und Velozählung—Viertelstundenwerte*. https://data.stadt-zuerich.ch/dataset/ted_taz_verkehrszaehlungen_werte_fussgaenger_velo/resource/8bb6b21f-e412-4710-a50f-26202b2d1ca3

swisstopo. (2020). *swissSURFACE3D Raster* [Dataset]. https://www.swisstopo.admin.ch/en/height-model-swisssurface3d-raster

Toparlar, Y., Blocken, B., Maiheu, B., & van Heijst, G. J. F. (2017). A review on the CFD analysis of urban microclimate. *Renewable and Sustainable Energy Reviews*, *80*, 1613–1640. https://doi.org/10.1016/j.rser.2017.05.248

Topham, G. (2022, July 19). Why do Britain’s roads melt and its rails buckle in heat? *The Guardian*. https://www.theguardian.com/business/2022/jul/19/why-does-britains-tarmac-melt-and-its-rails-buckle-in-heat

Tsoka, S., Tsikaloudaki, A., & Theodosiou, T. (2018). Analyzing the ENVI-met microclimate model's performance and assessing cool materials and urban vegetation applications–A review. *Sustainable Cities and Society*, *43*, 55–76. https://doi.org/10.1016/j.scs.2018.08.009

United Nations. (2019). *World Urbanization Prospects The 2018 Revision (ST/ESA/SER.A/420)*. United Nations, Department of Economic and Social Affairs, Population Division.

United Nations. (2022, July 19). *WMO warns of frequent heatwaves in decades ahead*. UN News. https://news.un.org/en/story/2022/07/1122822

Vahmani, P., & Jones, A. D. (2017). Water conservation benefits of urban heat mitigation. *Nature Communications*, *8*(1), 1072. https://doi.org/10.1038/s41467-017-01346-1

Van Wijk, W. R., Scholte Ubing, D. W. (1963). Radiation. In *Physics of plant environment* (pp. 62–101). North-Holland Pub. Co.

Wang, C., Wang, Z.-H., Kaloush, K. E., & Shacat, J. (2021). Cool pavements for urban heat island mitigation: A synthetic review. *Renewable and Sustainable Energy Reviews*, *146*, 111171. https://doi.org/10.1016/j.rser.2021.111171

Wang, K., Wan, Z., Wang, P., Sparrow, M., Liu, J., Zhou, X., & Haginoya, S. (2005). Estimation of surface long wave radiation and broadband emissivity using moderate resolution imaging spectroradiometer (MODIS) land surface temperature/emissivity products. *Journal of Geophysical Research D: Atmospheres*, *110*(11), 1–12. https://doi.org/10.1029/2004JD005566

Wang, L., & Li, D. (2021). *Urban Heat Islands during Heat Waves: A Comparative Study between Boston and Phoenix*. https://doi.org/10.1175/JAMC-D-20-0132.1

Weller, H. G., Tabor, G., Jasak, H., & Fureby, C. (1998). A tensorial approach to computational continuum mechanics using object-oriented techniques. *Computer in Physics*, *12*(6), 620–631. https://doi.org/10.1063/1.168744

Wong, N. H., Tan, C. L., Kolokotsa, D. D., & Takebayashi, H. (2021). Greenery as a mitigation and adaptation strategy to urban heat. *Nature Reviews Earth & Environment*, *2*(3), 166–181. https://doi.org/10.1038/s43017-020-00129-5

Yin, S., Peng, L. L. H., Feng, N., Wen, H., Ling, Z., Yang, X., & Dong, L. (2022). Spatial-temporal pattern in the cooling effect of a large urban forest and the factors driving it. *Building and Environment*, *209*, 108676. https://doi.org/10.1016/j.buildenv.2021.108676

Yu, C., & Hien, W. N. (2006). Thermal benefits of city parks. *Energy and Buildings*, *38*(2), 105–120. https://doi.org/10.1016/j.enbuild.2005.04.003

Yu, Z., Guo, X., Jørgensen, G., & Vejre, H. (2017). How can urban green spaces be planned for climate adaptation in subtropical cities? *Ecological Indicators*, *82*, 152–162. https://doi.org/10.1016/j.ecolind.2017.07.002

Zhang, Y., Murray, A. T., & Turner, B. L. (2017). Optimizing green space locations to reduce daytime and nighttime urban heat island effects in Phoenix, Arizona. *Landscape and Urban Planning*, *165*, 162–171. https://doi.org/10.1016/j.landurbplan.2017.04.009

Declaration of interests

☒ The authors declare that they have no known competing financial interests or personal relationships that could have appeared to influence the work reported in this paper.

☐The authors declare the following financial interests/personal relationships which may be considered as potential competing interests:

Graphical abstract

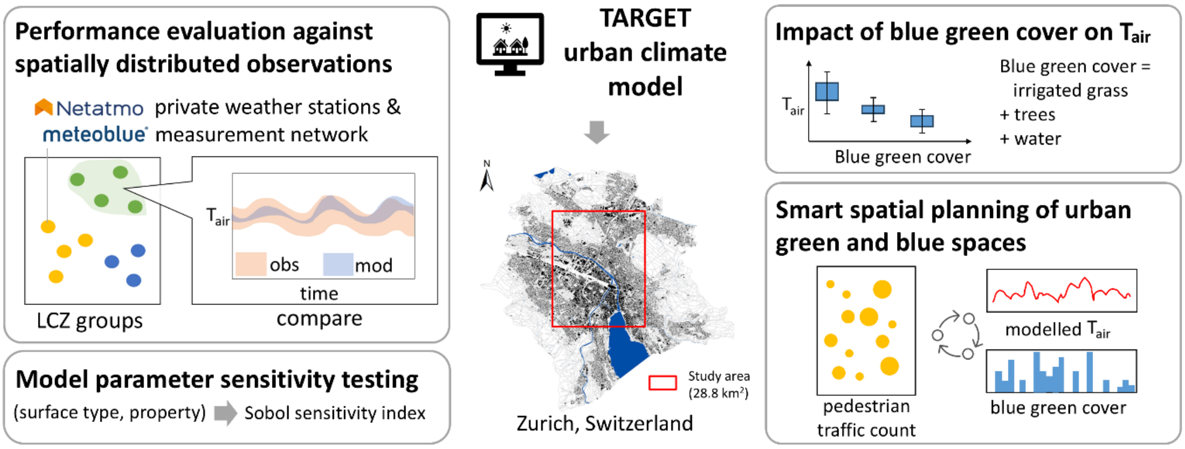

HIGHLIGHTS

- Investigating the applicability of an efficient urban climate model for planning liveable cities
- Good agreement between TARGET model results and spatially distributed private weather station data
- Sensitivity testing indicates key variables affecting urban heat: canyon shape and concrete parameters
- Substantial air temperature reduction (up to 5.2 °C) with increasing blue-green land cover across city
- Model coupling with pedestrian count data supports people-centric spatial planning of urban spaces

SUPPLEMENTARY INFORMATION

S1. TARGET modelling approach

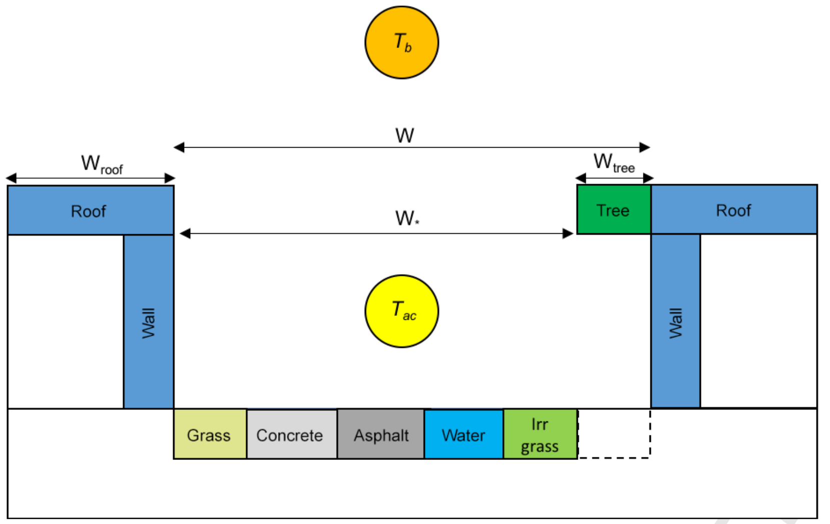

***Figure S2a**. Schematic of TARGET urban canyon set-up. Tac is the canopy layer air temperature, and Tb is the above-canopy air temperature, which is a uniform value across the whole domain. Wroof is the roof width, Wtree is the tree width, W is canyon width, and W*= W - Wtree. The surface beneath trees is assumed to be representative of canyon ground-level surfaces. Figure reprinted from Broadbent et al., The Air-temperature Response to Green/blue-infrastructure Evaluation Tool (TARGET v1.0): an efficient and user-friendly model of city cooling, Geoscientific Model Development, 2019, under the terms of the Creative Commons Attribution 4.0 License.*

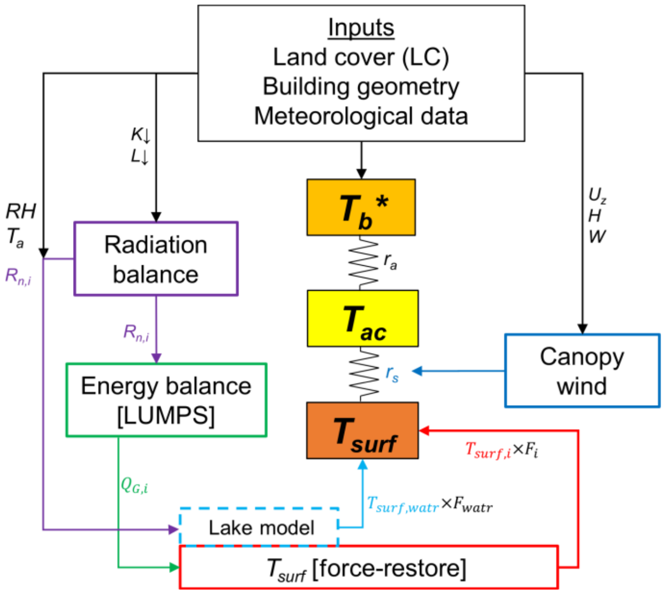

***Figure S1b**. Overview of approach used in TARGET. Tac is street-level (urban canopy layer) air temperature (C), Tb is the air temperature above the urban canopy layer (C), Tsurf,i is the surface temperature for surface type i, K is incoming shortwave radiation (W/m2), L is incoming longwave radiation (W/m2), Ta is reference air temperature (C), Rn is net radiation (W/m2), RH is relative humidity (%), Fi is the fraction of land cover type i (%), QH,i is the sensible heat flux for surface i from LUMPS (W/m2), QG,i is the storage heat flux for surface type i from LUMPS (W/m2), Uz is the reference wind speed (m/s), H is the average building height (m), W is the average street width (m), rs is the resistance from the surface to the canopy (s/m), and ra is the resistance from urban canopy to the atmosphere (s/m). Tb is the above-canopy air temperature, which is a uniform value across the whole domain. Figure reprinted from Broadbent et al., The Air-temperature Response to Green/blue-infrastructure Evaluation Tool (TARGET v1.0): an efficient and user-friendly model of city cooling, Geoscientific Model Development, 2019, under the terms of the Creative Commons Attribution 4.0 License.*

S2. Pictures of Netatmo stations and optional shield

Figure S3a. Netatmo private weather stations, consisting of an indoor and an outdoor module. Source: https://shop.netatmo.com/en-us/weather/smart-weather-station/weatherstation

Figure S2b. Shield for the outdoor module. Source: https://shop.netatmo.com/en-us/weather/accessories/weather-station-shield?s=shield

S3. List of parameters used for simulations

Table S3. *Parameter values used in simulations*

	Roof and wall	Road	Water	Soil	Concrete	Dry grass	Irrigated grass	Tree
α	0.15	0.08	0.10	n/a	0.20	0.19	0.19	0.10
ε	0.9	0.95	0.97	n/a	0.94	0.98	0.98	0.98
C ($\times 10^6$)	1.25	1.94	4.18	3.03	2.11	1.35	2.19	n/a

κ ($\times 10^{-6}$)	0.05	0.38	0.14	0.63	0.72	0.21	0.42	n/a
T_m	25.0	26.0	24.5	n/a	26.0	22.4	21.5	n/a
OHM [a_1, a_2, a_3]	[0.12, 0.24, -4.5]	[0.50, 0.28, -31.45]	n/a	n/a	[0.61, 0.28, -23.9]	[0.27, 0.33, -21.75]	[0.32, 0.54, -27.4]	[0.11, 0.11, -12.3]
α_{pm}	0.0	0.0	n/a	n/a	0.0	0.2	1.2	1.2
β	3.0	3.0	n/a	n/a	3.0	3.0	3.0	3.0

α is the surface albedo, ε is the surface emissivity, C is the volumetric heat capacity ($\times 10^6$) (J m^{-3} K^{-1}), κ is the thermal diffusivity ($\times 10^{-6}$) (m^2 s^{-1}), T_m is the initial ground temperature (°C), OHM [a_1, a_2, a_3] are LUMPS empirical coefficients, α_{pm} is the LUMPS empirical alpha parameter, and β is the LUMPS empirical beta parameter.

S4. List of case-specific constants used for simulations

Table S4. *Explanations and values of constants specific to Zurich case study*

Constant	Explanation	Value (m)
zavg	Average building height in domain	10.73
z_TaRef	Height of reference air temperature measurements	2.0
z_URef	Height of reference wind speed measurements	28.05

S5. Impact of meteorological input on modelling results

The study also investigated the impact of meteorological inputs from different meteorological stations. Data from Kloten station, which is located next to the Zurich airport, and the Fluntern station, which sits in a more urbanised area and is much closer to the study area, were compared.

As shown in Figure S6, with meteorological data from either station, TARGET replicated the temperature peaks well. However, it generated better results during the night with Fluntern data. Therefore, better agreement with observed data is achieved with Fluntern data, as indicated by the r-squared and error metrics. For the urban case, Fluntern has higher r-squared and lower errors. Although Kloten's r-squared is 0.01 better for the less urban case, Fluntern's error terms are considerably lower. Conformity with observed data is slightly better in urban areas than in less urban areas. As a result, Fluntern data were used as the default meteorological input in all simulations in this study.

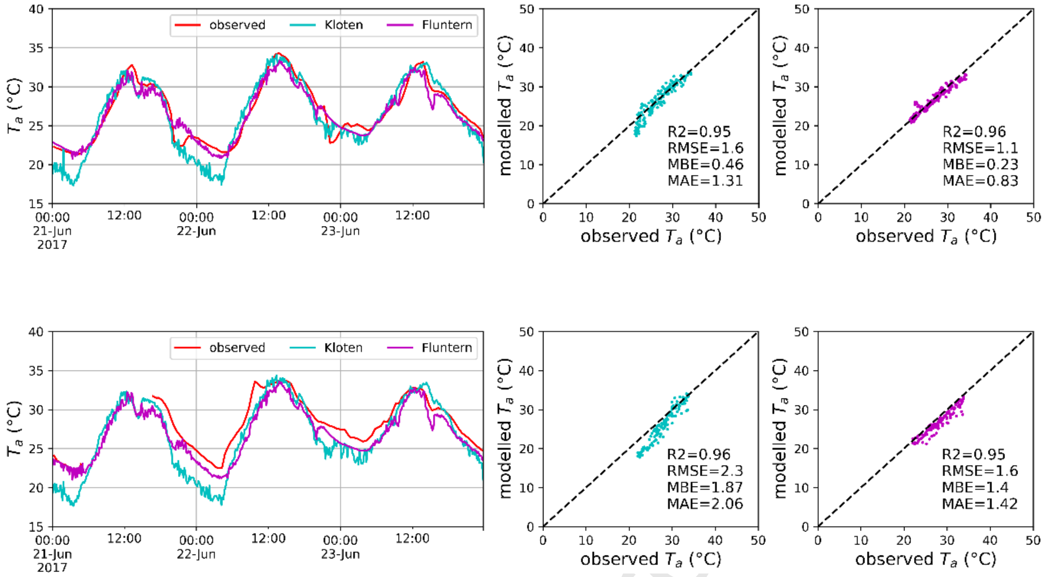

(a)

(b)

Figure S5. *Time-series comparison of Kloten and Fluntern results with Netatmo observed data, complemented with scatterplots for Kloten and Fluntern separately, for (a) an urban case and (b) a less urban case.*

Although not typically recommended for TARGET meteorological input, there are reasons why Fluntern achieved better results compared to Kloten. The Fluntern station is located right next to the study area, so its meteorological measurements might be more alike with the actual conditions in the region of interest. On the contrary, the Kloten station is farther away and is very likely to have different meteorological conditions due to the two hills between the station and the study area. Besides, located in the city, the Fluntern station measures a higher night-time incoming longwave radiation, capturing the night-time temperature better. TARGET does not account for warm air advection or heat generation from buildings due to energy use, so it is expected to have underestimated night-time temperature with meteorological data from a rural area like Kloten.

Testing of different meteorological inputs is encouraged for similar studies with TARGET. As TARGET forces the meteorological input to the whole simulation area, it is essential to find a meteorological station that can best estimate the temperature while conforming to TARGET's requirement of open space. In the future, TARGET may be improved to use data from multiple meteorological stations simultaneously, which means forcing spatially distributed meteorological data to the area of interest. This improvement will allow TARGET to generate more accurate results and potentially be applied to larger areas.

S6. Parameter sensitivity analysis results

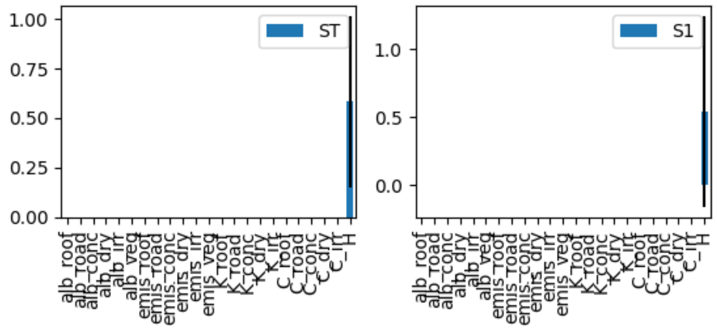

Figure S6a. Total and first order sensitivities for parameter sensitivity analysis including H/W.

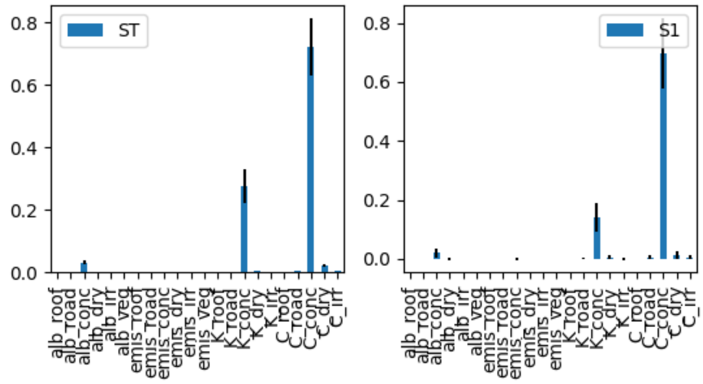

Figure S6b. Total and first order sensitivities for parameter sensitivity analysis excluding H/W.

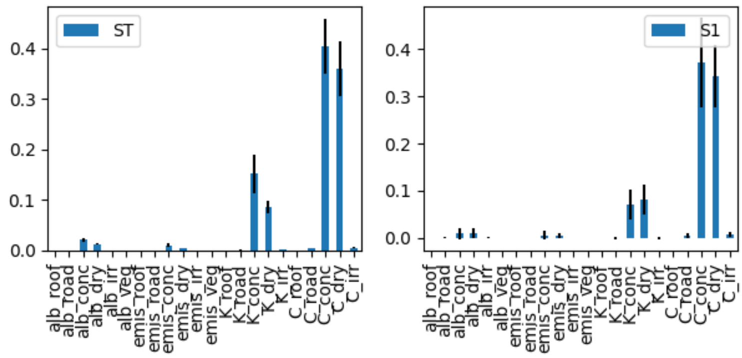

Figure S6c. Total and first order sensitivities for parameter sensitivity analysis excluding H/W, at 06:00.

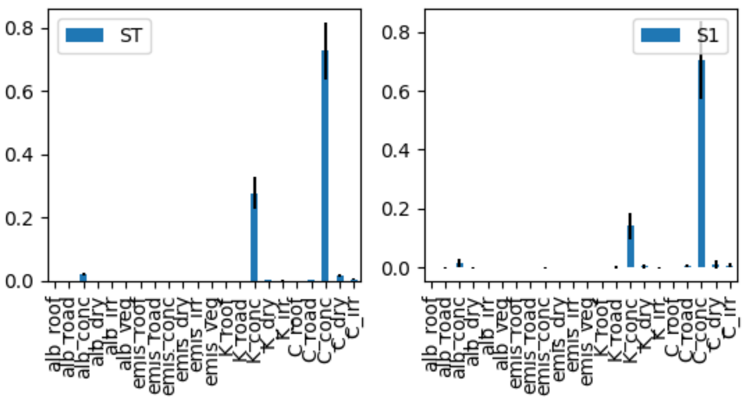

Figure S6d. Total and first order sensitivities for parameter sensitivity analysis excluding H/W, at 14:00.

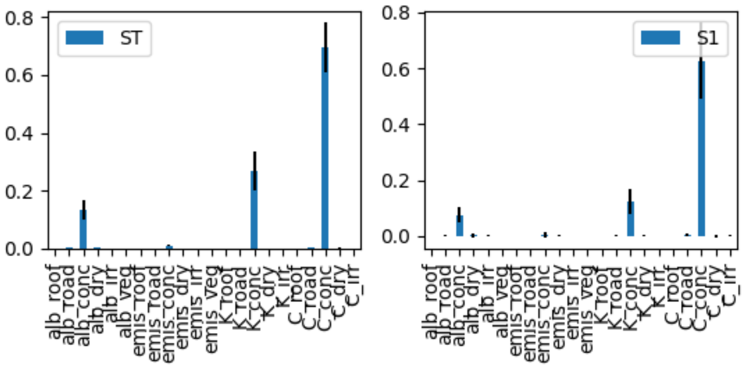

Figure S6e. Total and first order sensitivities for parameter sensitivity analysis excluding H/W, at 22:00.

Figure S6f. Extreme values for air and surface temperatures obtained in simulation results for parameter sensitivity analysis excluding H/W, average. Unit: °C

Min Ta	Max Ta	Min Ts	Max Ts
23.50	23.56	23.84	23.90

S7. Overall point-to-point comparison of modelled and observed air temperatures

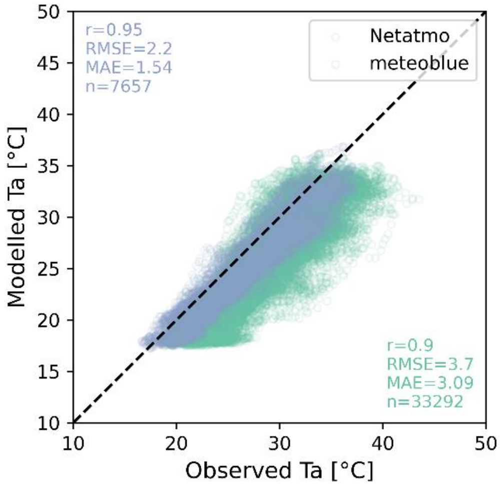

Figure S7. *Point-to-point comparison of observed and modelled air temperatures for all NetAtmo stations for the period 21/06/2017 00:00 – 24/06/2017 00:00.*